Weather and Climate Extremes 32 (2021) 100313

Contents lists available at ScienceDirect

Weather and Climate Extremes

journal homepage: http://www.elsevier.com/locate/wace

Understanding compound hazards from a weather system perspective

Jennifer L. Catto [a,*], Andrew Dowdy [b]

[a] College of Engineering, Mathematics and Physical Sciences, University of Exeter, North Park Road, Exeter, UK
[b] Climate Research Section, Bureau of Meteorology, Melbourne, Australia

ARTICLE INFO

Keywords:
Compound hazards
Weather systems
Extreme precipitation
Extreme winds
Extreme waves

ABSTRACT

Natural hazards such as extreme wind, rainfall and ocean waves can have severe impacts on built and natural environments, contributing to the occurrence of disastrous events in some cases. These hazards are often caused by weather systems such as cyclones, fronts and thunderstorms. Previous studies typically examine one type of hazard and/or one type of weather system, with some studies in recent years starting to focus on compound hazards. Here we systematically examine compound hazards (extreme precipitation, extreme wind gusts, and extreme waves) from a weather system typology perspective. Cyclones and fronts are identified automatically from ERA-Interim reanalysis data, and thunderstorm events are based on lightning observations from 2005 to 2015, defining the study period. Relationships are examined over this period between the different compound hazard types and the weather system types, globally for different seasons. Most of the individual and compound hazards are most likely to be associated with the front-only or cyclone and front weather system types, while in the tropics, most hazards are strongly associated with the thunderstorm-only type. Despite being less frequent than the double weather system types, the triple weather system type shows comparable importance for many of the hazards, and especially the triple hazard. Individual case studies are examined using this compound event framework. It is intended that a greater understanding of compound hazards and the weather systems that cause them in regions throughout the world will help lead to improved preparedness and disaster risk reduction, given the importance of this for our rapidly changing world.

1. Introduction

Extreme precipitation, extreme wind gusts, and extreme ocean waves are types of natural hazards that can cause significant impacts. These individual hazards may also occur at the same time to produce compound hazards, with increased impacts for a given region. Such compound hazards are of great interest to emergency management and the insurance industry (Zscheischler et al., 2018). Additionally, certain features of weather systems that cause these hazards can combine in such a way as to increase the risk of experiencing a hazard (e.g., Dowdy and Catto, 2017). In this study we will quantify the frequency of compound hazards and use the weather system typology framework developed in Dowdy and Catto (2017) to understand their interrelationships.

A compound weather or climate event can be considered as the combination of multiple drivers and/or hazards that contribute to societal or environmental risk (Zscheischler et al., 2018), and would include: (1) two or more extreme events occurring simultaneously or successively, (2) combinations of extreme events with underlying conditions that amplify the impact of the events, or (3) combinations of events that are not themselves extremes but lead to an extreme event or impact when combined (Special Report on Extremes, SREX; Seneviratne et al., 2012). Here we are specifically considering compound extremes (as a subset of the broader compound event definition) for the case when two or more individual extreme events occur at the same time and place. Here these hazards are extremes of precipitation, wind gusts and ocean waves.

The risks of experiencing compound extremes is strongly affected by the dependence of the variables in question (Zscheischler and Seneviratne, 2017) with a much higher likelihood of occurrence when the variables are highly correlated compared to more independent (uncorrelated) variables. This is particularly true for compound hazards such as extreme wind speeds and wave heights occurring in a given region, given the direct physical link between wind speed and locally generated wave activity (as distinct from swell waves that may propagate from source regions further away).

Recent studies have looked at different types of compound hazards

* Corresponding author.
E-mail address: j.catto@exeter.ac.uk (J.L. Catto).

https://doi.org/10.1016/j.wace.2021.100313
Received 29 May 2020; Received in revised form 8 February 2021; Accepted 9 February 2021
Available online 28 February 2021

for various regions of the world using a number of methods (e.g. Zheng et al., 2014; Martius et al., 2016; Liu et al., 2016; De Luca et al., 2020). Martius et al. (2016) found, using reanalysis data, that up to 50% of extreme precipitation and wind events occurred jointly in some regions, such as the tropical cyclone regions of the Northern Hemisphere (NH) and Southern Hemisphere (SH), and along the west coasts of Europe and North America. The high frequency of co-occurring wind and precipitation events is also seen in other datasets, (Owen et al., 2021). Over Europe Martius et al. (2016) found that two examples of concomitant extreme events were associated with named windstorms Dagmar and Xynthia (Liberato et al., 2013), with the extreme wind area being much larger than the extreme precipitation area within these systems, while Owen et al., 2021 find that a large proportion of co-occurring extremes can be linked to extratropical cyclones. In the Mediterranean region large-scale wind and precipitation compound extremes (1 000 km extent and 3 days duration) have also been linked to extratropical cyclones (Raveh-Rubin and Wernli, 2015).

The co-occurrence of heavy precipitation and storm surge events, which are influenced by winds and waves, increases the chance of experiencing high inland water levels in the Netherlands (van den Hurk et al., 2015), although astronomical tides can also play an important role for very high water levels. For Australia, Wu et al. (2018) mapped the risk of compound hazards from extreme precipitation combined with storm surge events, which are important for coastal flood risk factors. The analysis of the different synoptic-scale weather systems associated with the compound hazard types revealed that tropical cyclones were responsible for most of the compound hazards (precipitation and storm surge together) along the northern coast, and in the south extratropical cyclones were related to the compound hazards, while fronts were the main cause of the extreme precipitation. The risk of compound flooding events has also been mapped for the future projected climate in Europe, based on the co-occurrence of high sea levels and precipitation resulting in large runoff, finding significant regions of emerging high risk along parts of coastal Europe (Bevacqua et al., 2019, 2020).

Extreme wave heights can be important for shipping and other offshore activities such as oil exploration (Bell et al., 2016), and are frequently associated with extratropical cyclones (O'Brien et al., 2018). The likelihood of an extreme wave height event in the North Sea region depends strongly on the direction of the wind and the fetch across the open ocean (Bell et al., 2016), and more often occur in the cold conveyor belt part of the cyclone. At the coasts in particular, when extreme waves, wind, and precipitation occur simultaneously, this could have hugely damaging consequences through the combined storm surge, wind damage and flooding (e.g. hurricane/superstorm Sandy). Ye and Fang (2018) considered tropical cyclones over China and found that the joint return period of extreme winds and precipitation calculated using copula functions gave a better correlation to economic losses than consideration of the individual return periods. They suggested that an even more comprehensive hazard estimate could be found by including storm surge and wave data.

As well as extratropical cyclones, fronts have also been found to be associated with extreme precipitation, particularly in the mid-latitudes where up to 90% of large-scale extreme precipitation events (99th percentile events) can be linked to fronts (Catto and Pfahl, 2013), and even rarer extreme events are also linked to fronts (Kunkel et al., 2012). Many highly ranked compound extreme events on the Iberian peninsula can be linked to atmospheric rivers, also indicating a role for fronts (Hénin et al., 2020).

Dowdy and Catto (2017) considered cyclones (both in the mid-latitudes and the tropics), fronts, and thunderstorms yielding seven combined weather system types: cyclone only; front only; thunderstorm only; cyclone and front; cyclone and thunderstorm; front and thunderstorm; and cyclone, front and thunderstorm. The combination of cyclone, front and thunderstorm all together, while occurring the least often of the 7 storm types, was found to have the highest increased risk of producing an extreme precipitation or extreme wind event (Dowdy and Catto, 2017). Utsumi et al. (2017) also examined cyclones and fronts in combination with each other, including associated rainfall characteristics, finding that over the storm track regions, taking cyclones and fronts and their combinations accounted for up to 90% of annual precipitation and almost all the extreme precipitation.

While compound extreme events (precipitation and winds) in the mid-latitudes and Mediterranean region are strongly associated with cyclones (Raveh-Rubin and Wernli, 2015; Martius et al., 2016), there are questions remaining about the importance of other systems such as fronts and smaller-scale processes (Raveh-Rubin and Wernli, 2015), including thunderstorms. There are also large knowledge gaps around how compound hazards relate to different weather system types, as is a focus of this study, noting that this has not been examined in previous studies. A number of key questions that this study aims to examine are as follows:

1. What is the seasonal occurrence frequency of the compound hazards and the weather system types?
2. How do the compound hazard types relate to the weather system types?
3. Which weather systems are the most important for the compound hazards and how does this vary spatially?
4. How does the likelihood of a compound extreme occurrence vary for different weather system types?

While local conditions are important for setting the impact of the compound hazards, the global analysis performed here of the occurrence of the extreme hazards and their chance of occurring associated with different weather systems is a vital step in understanding such events. Understanding the global risk of compound hazards of extreme precipitation, wind, and waves and how this relates to different weather systems will contribute to enhancing the predictability of such high impact events, and improving disaster risk reduction strategies both for present conditions and potential future scenarios.

2. Materials and methods

2.1. Data

The ERA-Interim reanalysis product (Dee et al., 2011) from the European Center for Medium-range Weather Forecasts (ECMWF) has been used for much of the analysis in this study, including the identification of extreme events, and identification of fronts and cyclones. The data from 2005 to 2015 have been used at 6-hourly temporal resolution, on a 0.75° regular grid.

The precipitation data used are consistent with Dowdy and Catto (2017), and are taken as the 6-hourly accumulations at lead times of 6 and 12 h from ERA-Interim, which are calculated from the Integrated Forecasting System (IFS) forecasts from 00 UTC and 12 UTC. We acknowledge that there can be potential issues with using such forecast data. However, Pfahl and Wernli (2012) show that ERA-Interim extreme precipitation events match well in time with those from the satellite based CMORPH dataset.

Similarly, the wind gust data are the maximum 10-m gusts in the preceding 6 h as provided from the ERA-Interim reanalysis dataset, as used in Dowdy and Catto (2017). The wave height data are also as provided in the ERA-Interim reanalysis, for the significant wave height (SWH) representing the mean wave height of the highest third of the wave data, noting that the ERA-Interim reanalysis wave heights are simulated in the IFS based on the WAM (Wave Modeling Group) approach (Komen et al., 1994). Although the focus of this study is on weather systems and hazards that occur concurrently in a given region, which is more conducive to accounting for waves generated by local winds, it is also noted that some swell waves can propagate from remote source regions such as has been examined and mapped throughout the world in various previous studies (e.g., Semedo et al., 2011). The

compound event framework used here (i.e., based around the simultaneous occurrence of different types of extreme events) may preferentially favour locally generated wind waves for some regions of the world, while noting that swell waves will have larger influences in some other regions, as is examined in some sections of this study that map the strength of relationship between extreme winds and wave heights at a given location.

2.2. Identification of hazards

The seasonal 98th percentiles are used for indicating extreme precipitation, wind gusts and wave height. The data are separated into 3-month seasons, and here we focus on December, January, and February (DJF) and June, July, and August (JJA) to highlight the extremes of the seasonal cycle. Winter is referred to throughout this study as DJF for the NH and JJA for the SH. The grid box 98th percentile is calculated from all of the seasonal data for the 11 years from 2005 to 2015. For the precipitation data, this includes any times with zero precipitation. Events are then identified at each grid point if the value is above the 98th percentile for that season. The 98th percentile thresholds are shown for each hazard and season in Fig. S1. The threshold magnitudes vary widely, but are generally consistent with the pattern of the mean that we would expect. For example, during winter, the highest 98th percentile thresholds for precipitation (Fig. S1d) are over the mid-latitude storm tracks, whereas in summer (Fig. S1a), there are higher thresholds over the intertropical convergence zone (ITCZ). There are regions in both summer and winter where the 98th percentile threshold for precipitation is below 1 mm. These are typically in the subtropical high regions. For the wind gusts, the highest thresholds are seen in the mid-latitudes over the ocean, with the seasonal cycle very prominent in the NH. The wave height thresholds follow a similar pattern to the wind gusts.

The three separate hazards are combined to produce the joint hazards by applying criteria to the spatial and temporal co-occurrence. We have opted to define a co-occurring hazard as one that has two (or more) different hazards occurring at the same time or one time-step (6 h) apart, and in the same grid box or the surrounding eight grid boxes. This accounts for the slight spatial offsets of the hazards that are clearly related to the same weather system, and also the movement of that weather system, and gives a larger number of hazard events overall to increase the sample size and the robustness of the results. The sensitivity to the choice has been tested by applying different time relaxations (0 h–± 18 h), and different spatial search areas (exactly coincident to within a region of 49 grid boxes, i.e. ±3 grid boxes). We end up with 7 different hazards, extreme precipitation-only, extreme wind-only, extreme waves-only, extreme precipitation and wind, extreme precipitation and waves, extreme wind and waves, and the triple hazard of extreme precipitation, wind, and waves combined. The results of the sensitivity testing are shown in the supplementary material (Fig. S2). In general, the larger the area and the larger the time relaxation, the more hazards are identified. We acknowledge that the relaxation in space and time of the matching criteria may also increase the co-occurrence of hazards that are not directly related (e.g. associated with different weather systems), but the method used here is selected based on considering these factors including the variations shown in the supplementary material. Extreme precipitation is the hazard that is most likely to occur without another hazard close by in space and time, which can be seen as the criteria are expanded. Martius et al. (2016) tested their methodology for investigating the co-occurrence of extreme events by relaxing the matching criteria to consider neighbouring grid points on the same day, or the same grid point but shifted in time by one day. Raveh-Rubin and Wernli (2015) find that in the Mediterranean region, the extreme precipitation peak precedes the wind gust peak by about 12 h.

There are some regions where extreme precipitation events are hard to detect due to the fact that precipitation itself occurs less frequently than the 2% of times required to find a 98th percentile value (i.e. over parts of North Africa). This region can be seen as blank in Fig. 2a. It is important to note that even though we are using the 98th percentile to define an extreme, because of the expanded area for matching of the hazards, the frequency of the hazards can be above 2%. At each time and grid box, we are checking for the existence of a hazard within 9 grid boxes. The total frequency of any extreme precipitation event (including the compound events), any extreme wind gust event, and any extreme wave event are shown in the supplementary material (Fig. S3), and the proportion of these associated with the different hazard types are shown in Supplementary Figs. S6–S11.

To test whether the co-occurrence of the hazards could be due to random chance, we have devised a method that finds the probability of hazards co-occurring using the individual hazards from different regions. To maintain the spatial autocorrelation of the extreme events, we extracted a 30° by 30° region from the North Atlantic basin for precipitation, the North Pacific basin for winds, and the Southern Ocean for waves, for all times in the dataset. The algorithm that calculates the frequency of the seven hazard types was applied to these data as though they all came from the same place. The need for this method arises from the spatial and temporal criteria for matching extremes. A table showing the mean frequency of each randomly matched hazard type is shown in the supplementary material, along with alternative versions of Figs. 1 and 2 with only the values above these thresholds retained (Figs. S4 and S5).

2.3. Identification of weather system types

Seven weather system types have been identified using the same method as Dowdy and Catto (2017) and are defined at each grid point. The method is described in detail in that paper, so here we give a brief account.

Atmospheric fronts are identified using a thermal front parameter method from Berry et al. (2011) and based on Hewson (1998). The thermal front parameter is calculated as $TFP(\theta_w) = -\nabla|\nabla\theta_w|.(\nabla\theta_w/|\nabla\theta_w|)$, where θ_w is the wet bulb potential temperature at 850 hPa. Where the *TFP* is below a certain threshold, the field is masked out. In the remaining field, where the gradient of *TFP* is zero, a frontal point is identified. This places the front at the leading edge of the frontal zone (see Hewson, 1998, for a schematic). Once the frontal points are identified they are linked into contiguous fronts using a line-joining algorithm, and both warm and cold fronts are included. Fronts that are shorter than 250 km are excluded.

Cyclones are identified using an updated version of the Wernli and Schwierz (2006) method (Pfahl and Wernli, 2012). This defines cyclones as the area within the outermost closed contour of mean sea level pressure (MSLP) around a low center. The contour intervals of MSLP are 0.5 hPa. This allows a cyclone area of influence to be defined without the need for further assumptions about cyclone size. Additionally, as some tropical cyclones are not well-resolved at the scales of current reanalyses, the cyclone data are supplemented by the addition of global tropical cyclone data from the International Best Track Archive for Climate Stewardship (IBTrACS; Knapp et al., 2010).

The thunderstorm data are defined following the method used in Dowdy and Catto (2017). Observations of lightning strokes are obtained from a ground-based network of lightning detection sensors, the World Wide Lightning Location Network, WWLLN (WWLLN; Virts et al., 2013). The lightning data are gridded on the same grid as used for the cyclone and front data (i.e., 6-hourly time steps and 0.75° grid spacing), noting that the WWLLN observations are available at finer spatial and temporal resolutions than are the focus of this study. Grid-cells containing thunderstorms are then identified based on two or more lightning strokes observed within the 0.75° × 0.75° region and 6-h period represented by a particular grid-cell and time step, noting that a single lightning flash can often contain multiple lightning strokes and that the vast majority of thunderstorms produce many (e.g., 10 or more) lightning flashes. Consequently, although the detection efficiency of the WWLLN sensor

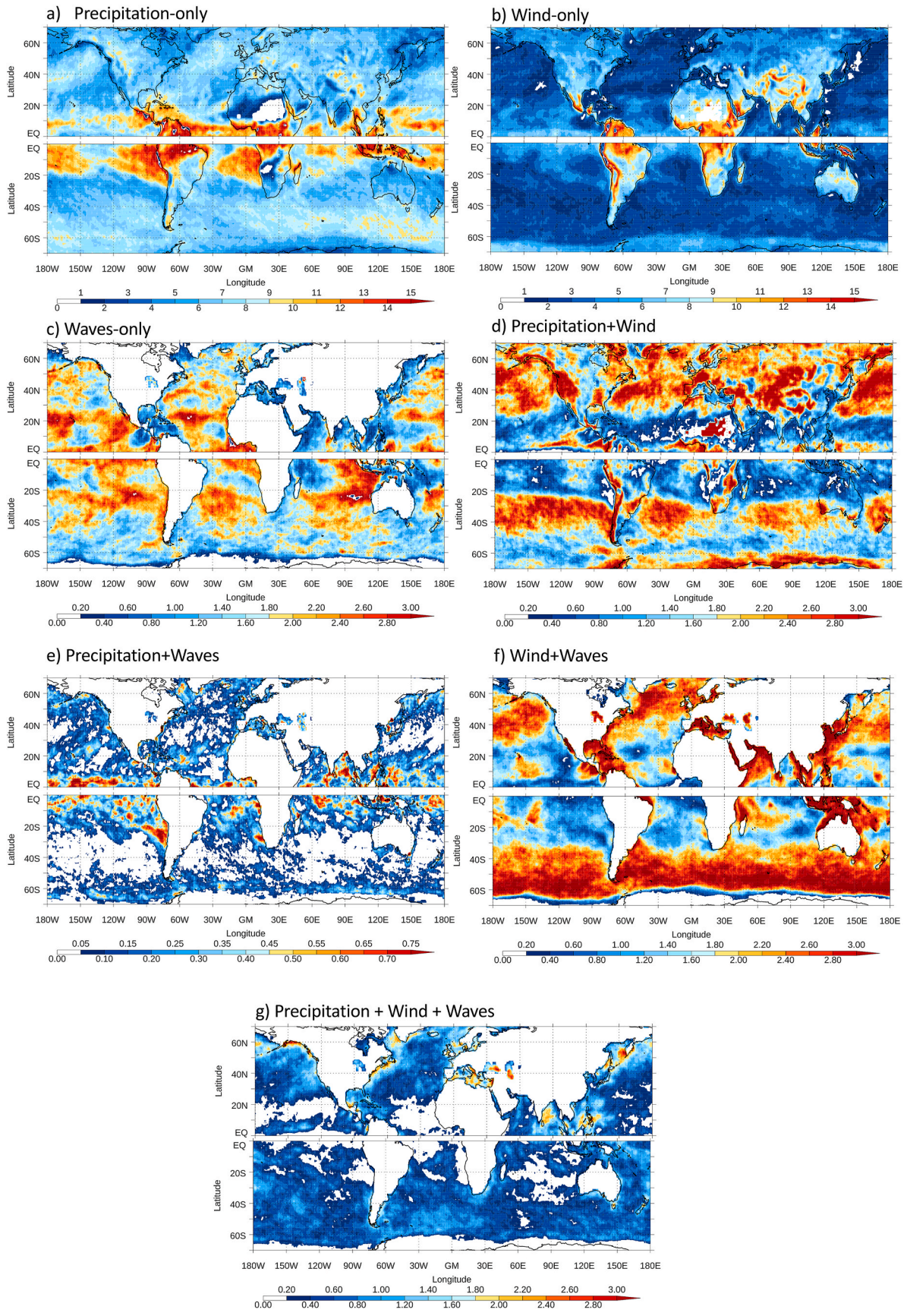

Fig. 1. Winter seasonal mean frequency (% times) of 98th percentile hazard types: (a) extreme precipitation-only, (b) extreme wind-only, (c) extreme waves-only, (d) extreme precipitation and wind, (e) extreme precipitation and waves, (f) extreme wind and waves, and (g) extreme precipitation, wind and waves.

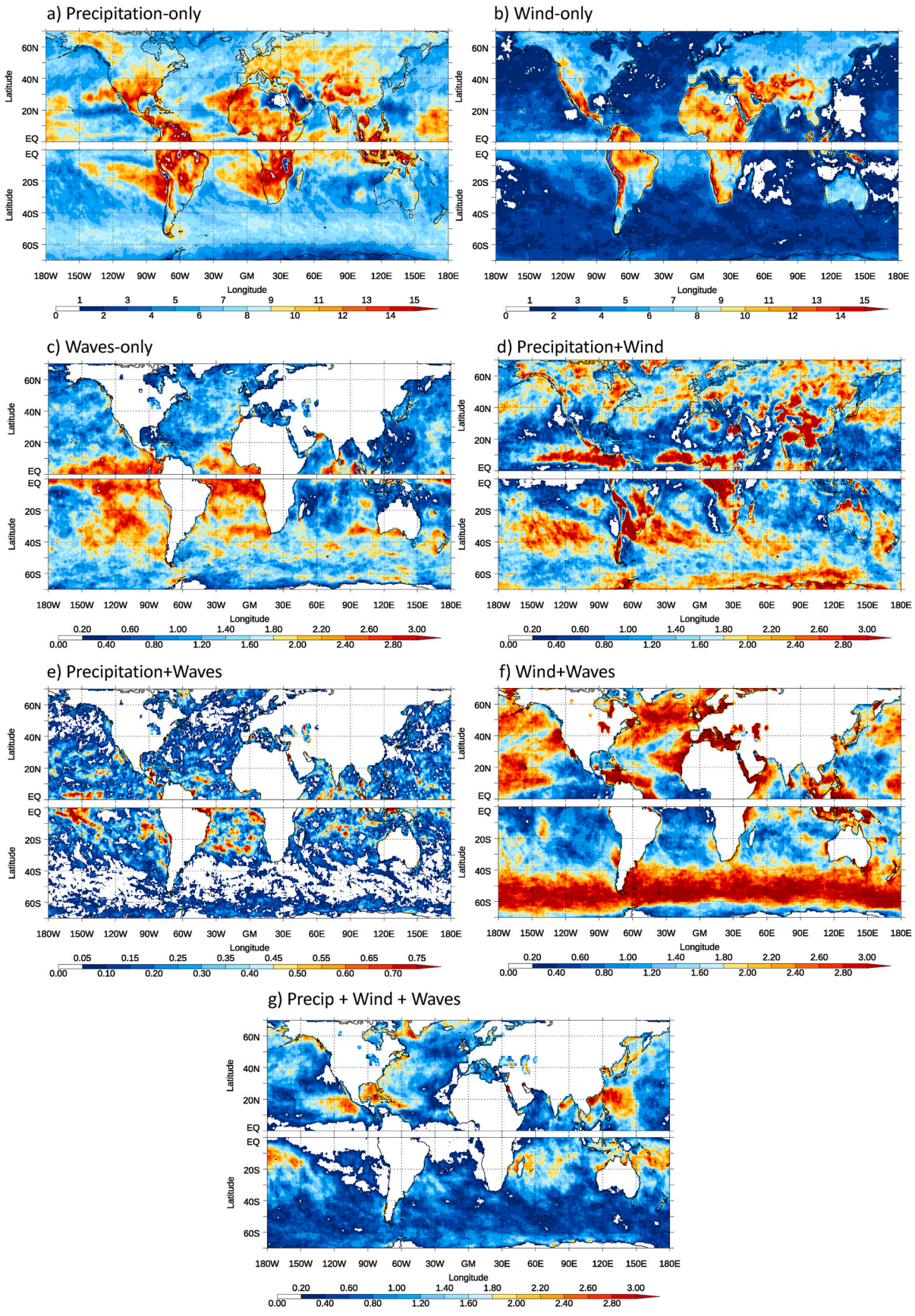

Fig. 2. As Fig. 1 but for summer.

network can be of the order of 10% in some regions (Virts et al., 2013) this approach will provide a good representation of thunderstorms that produce a reasonable number of lightning flashes, acknowledging that some of the weaker systems may not always be counted. This approach is intended to provide an indication of deep convective storms at a location within a grid cell region and 6-h time period.

Each individual weather system type is expanded in size by three grid boxes (i.e. 2.25°) in all directions. This takes into account the area of influence of the features, and the expansion was found by Dowdy and Catto (2017) to give a good representation of the matching of weather systems with extreme precipitation and wind events (see Dowdy and Catto (2017) Supplementary Fig. 1). Due to the convergence of the meridians, there is some difference in the size of the expanded area at different latitudes, however this difference is largest at the highest latitudes, which are not included in this study. The combined weather system types are created by identifying times when more than one of the individual expanded weather system types is located at the same grid box. This gives the seven weather system types of cyclone only (CO), front only (FO), thunderstorm only (TO), cyclone plus front (CF), cyclone plus thunderstorm (CT), front plus thunderstorm (FT), and cyclone plus front plus thunderstorm (CFT). To be clear, there may be cyclones that have a front associated with them, so in this case the grid points of the cyclone region without a front would be classed as CO and those with a front would be CF (i.e., the classification is done on a grid point basis rather than a system basis).

2.4. Linking hazards and weather system types

The hazard is associated with the weather system if they occur at the same time at the same grid box. Given the expanded size of the weather system and the criteria for the matching of the hazards, this accounts for the movement of the weather systems and the sometimes distant influence of the weather systems on the precipitation, wind and waves.

Our analysis yields the frequency of the individual hazards (i.e. when there are no other hazard types within the time and space co-occurrence criteria) and the joint hazards at each grid box. For the maps the frequency is calculated at each grid box as the percentage of 6-hourly times that the features can be identified at that grid box. For the zonal means, the grid box frequencies are averaged. We also find the frequency of each hazard associated with each weather system type in the same way, and the proportion of the hazards associated with each weather system type, calculated by dividing the frequency of the hazard with each weather system type by the frequency of the hazard. We can also identify the weather system type (including concurrent weather systems) most commonly associated with each hazard (including compound hazard types). Not all hazards are linked to a weather system type, especially in regions where the frequencies of the weather system types are low.

3. Compound hazards

3.1. Frequency of compound hazards

Figs. 1 and 2 show the maps of the frequency of the individual hazards (i.e. an extreme in only one of precipitation, wind or waves, which will be referred to as precipitation-only, wind-only, and waves-only), as well as the compound hazards, for winter and summer respectively, as a percentage of all 6-hourly times from 2005 to 2015.

During winter we can see that the extreme precipitation-only events occur most frequently of all the hazards (Fig. 1a), up to 9% of the time in the mid-latitude storm track regions, and 15% of the time over some subtropical and tropical regions, including the Maritime Continent. Extreme wind-only events occur between 2 and 5% of the time over the oceans and with higher frequencies over equatorial land and over high orography (Fig. 1b). The extreme waves-only occur between 1 and 4% of the time over the oceans, with slightly higher values seen in the mid-latitudes than the high latitudes (Fig. 1c). Fig. S4 indicates that these frequencies could be by chance, as they are not higher than the frequency from random matching.

In the NH, joint extreme precipitation and wind events (Fig. 1d) occur more frequently north of 20°N, with the highest frequency for a broad-scale region occurring in the northwest Pacific storm track region up to about 3% of the time. There are some regions over land that have high frequencies of joint precipitation and wind extremes, such as over California and the Pacific coast of North America, the Iberian Peninsula and parts of northwestern Europe, and northwest Africa, and these are all considered significant according to Fig. S4d. Fig. 1d also highlights a region along the Equator where extreme wind and precipitation events occur more often than in other parts of the world, noting the relatively weak wind speeds in this region (often referred to as the 'doldrums' or 'horse latitudes') associated with the convergence of the trade winds and the ITCZ.

In the SH winter the highest frequencies of the joint wind and precipitation extremes (Fig. 1d) generally tend to occur between 20 and 40°S, with maxima to the west of South America, and between Australia and New Zealand, and a broad-scale minimum in a zonal band between about 45 and 60°S. There are also relatively high frequencies indicated around the Antarctic coast. Joint wind and wave hazards are common on the west coasts of the SH continents. Some of these features look similar to the results of Martius et al. (2016), but it must be taken into account that here our joint precipitation and wind events actually exclude the cases when the triple hazard (joint precipitation, wind and wave) events occur (Fig. 1g). These triple hazards further highlight the high frequency of compound events over the northwest Pacific, the west and east coasts of North America, Scandinavia, the Mediterranean, and parts of the southwest Pacific. These patterns of high frequency of compound events are broadly consistent with the frequency of co-occurring precipitation and wind events seen in the same regions in Martius et al. (2016) and Owen et al., 2021 and are significant according to our testing method. The triple hazards also occur with relatively high frequency around parts of the Maritime Continent in the NH and in the Bay of Bengal.

Joint extreme precipitation and wave events (Fig. 1e) are typically less frequent than the triple hazard and could easily be found by chance (see Supplementary Fig. S4), although they follow a similar pattern of spatial distribution. This highlights that when there is a joint precipitation and wave event, it is more likely to be associated also with extreme winds than only associated with extreme precipitation. This is due to the strong relationship between extreme winds and waves and the physical driving of the waves by the winds. It is possible that during the joint precipitation and wave events there are strong winds occurring, but they do not reach the threshold to be defined as extreme. It is also possible that the waves on these occasions are swell waves from further afield and therefore unrelated to the precipitation at the same grid point.

Joint wind and wave events (Fig. 1f) are very frequent over most of the Pacific and Atlantic Oceans, and over the Mediterranean, with a very strong zonal band throughout the SH between about 35 and 60°S with values above 3%. There are also some localized regions with values higher than this, including near Central America, northern Australia, the northwest Pacific and the Bay of Bengal. This indicates that winds and waves are strongly linked, as discussed above in relation to the relatively low values in Fig. 1e, and these frequencies would not be found by chance (Fig. S4f). The regions where the dependency of these two extremes is relatively low, for example near the Equator and parts of the subtropical oceans, shows where the extreme waves are not so often driven by local winds, but can be more strongly driven by swell coming from remote regions (e.g. as discussed by Semedo et al., 2011).

In the summer (Fig. 2) the extreme precipitation-only (Fig. 2a) and extreme wind-only (Fig. 2b) events occur most frequently over large parts of the continents, and these frequencies over land are mostly larger than would be found by chance (Figs. S5a and b). There is a broadly similar frequency to the winter season of the extreme waves-only and the double hazards (Fig. 2c–f). However, the joint extreme precipitation and wind events (Fig. 2d) do not exhibit the large maxima in the

extratropical storm tracks that are seen in winter, although their frequencies are still larger than would be found by chance. The dependence between the extreme wind and extreme waves is slightly higher in summer (Fig. 2f) than winter (Fig. 1f). The triple hazard (i.e. the simultaneous occurrence of extreme precipitation, winds, and waves) occurs more frequently in summer than winter (cf Figs. 2g and 1g). This is especially evident in the regions that experience tropical cyclones, such as to the west of Central America, in the Caribbean and the Gulf of Mexico, and in the Indian Ocean, around the north of Australia, and the tropical southwest Pacific. In the mid-latitudes the frequency of the triple hazards is not as high as for lower latitudes but with occurrence frequencies somewhat higher than the winter season in general, particularly in the NH with frequencies in the range 1–3%, and where they do occur they are not likely to be found by chance.

The large-scale mean frequency of the different hazards is shown in Fig. 3 for mid-latitude and tropical land and ocean regions separately for the NH and SH. Extreme precipitation-only and extreme wind-only are the most frequent, and these both occur more frequently over land than over the ocean as can be seen in the previous maps. There is a large seasonal variation in the frequency of extreme wind-only, with much greater frequency during summer in the NH. The double hazard of extreme wind and waves occurs on average more frequently than extreme wave-only events, and more in the winter season (suggesting a link with extratropical cyclones).

4. Seasonal frequency of weather system types

In order to better understand the causes of the various different compound hazard types, the meteorological causes of the events are examined here using a weather system typology. As a first step to quantifying the link between the hazards and the meteorology, we here present the seasonal frequencies of the seven weather system types defined by Dowdy and Catto (2017).

During winter (Fig. 4), the CO type occurs up to 40% of the time in the peak storm track regions of the North Pacific, North Atlantic, and around 60°S. FO has a similar maximum frequency of occurrence that covers a larger area of the two hemispheres, particularly for some mid-latitude oceanic regions. The maxima lie on the equatorward side of the main storm tracks (indicated by the CO maxima and as expected due to the typical structure of frontal cyclones with the fronts on the equator side of the cyclone) and to the east of Australia in the South Pacific Convergence Zone (SPCZ). TO occurs mainly in the tropics during winter, over the Maritime Continent, South America, and Africa, and the northern ITCZ. There is also a band of TO across the Kuroshio current region, the Gulf Stream, and in the Mediterranean, as well as similar mid-latitude regions near the east coasts of the three SH continents. The CF type has the highest maximum frequency of the joint weather system types, occurring up to 30% of the time in the mid-high latitudes, mainly in the storm track regions. CT and FT occur either in the tropics or subtropics, or over regions of warmer waters such as the Mediterranean. The triple weather system type shows a clear pattern of occurrence with distinct maxima near the coasts of continents in each hemisphere and adjacent maritime regions, as well as in the Mediterranean.

During summer (Fig. 5) the frequency of CO, FO and CF is generally lower than in the winter, although they follow similar broad-scale patterns. TO occurs very frequently over tropical and subtropical land regions as well as the Maritime Continent (e.g. more than 75% of the time over the Maritime Continent, and over tropical land in Africa and North and South America). There are also relatively large frequencies of TO in the convergence zones of the tropical oceans and over other, higher latitude land regions. CT occurs most frequently in the tropical cyclone regions in both hemispheres, as well as over North America and the Eurasian continent, while FT has higher frequency of occurrence over some parts of the lower mid-latitudes, such as over the Gulf Stream. The triple weather system type (CFT) occurs most frequently over land in general, which is somewhat different to the case for winter. Furthermore, it also occurs relatively frequently in mid-latitude regions to the east of the continents in both hemispheres, which is more similar to the case for winter. In general, the thunderstorm-related weather system types (i.e., TO, CT, FT, and CFT) are much more frequent over land during the summer, associated with the increased heating and thermodynamic instability.

5. Relation between compound hazards and storm types

In order to understand the meteorological causes of the compound hazards, in this section we link the hazard events with the weather system types. First we demonstrate how these features link using exemplary case studies.

5.1. Case studies

Hurricane Sandy was a huge storm that occurred in 2012 and caused severe damage to parts of eastern North America including New York City. Much of this damage was associated with flooding from storm surges, exacerbated by the heavy precipitation. The storm evolution was from a tropical cyclone that had undergone extratropical transition (Galarneau Jr. et al., 2013). Fig. 6 shows the evolution of the storm from

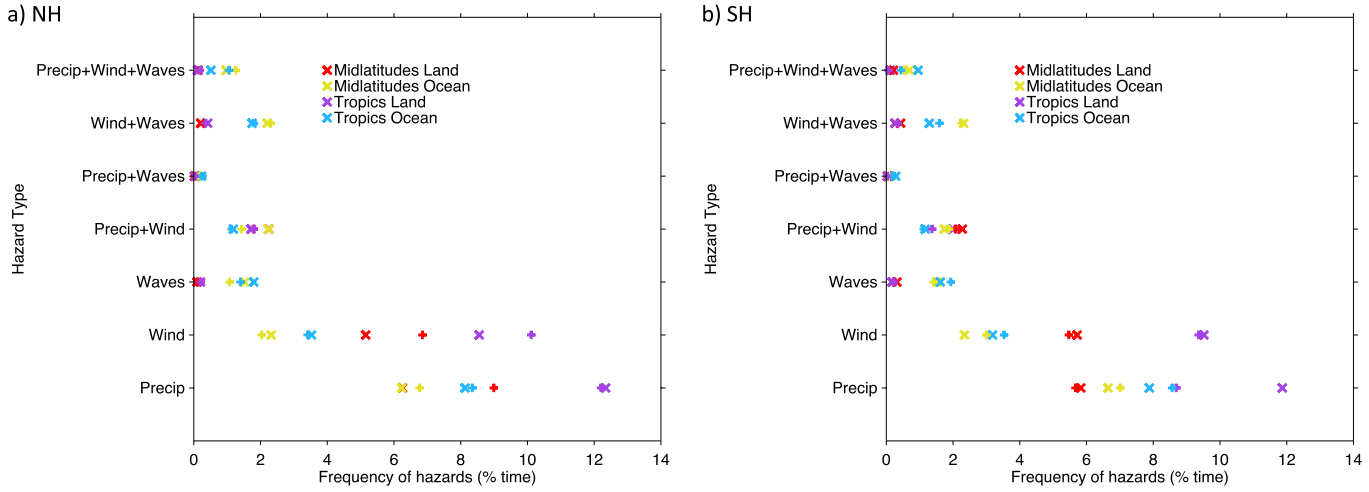

Fig. 3. Mean frequency of hazards over the mid-latitude (30–70°) land regions, mid-latitude ocean regions, tropical (Equator to 30°) land regions, and tropical ocean regions for DJF (crosses) and JJA (plus signs) for (a) NH and (b) SH.

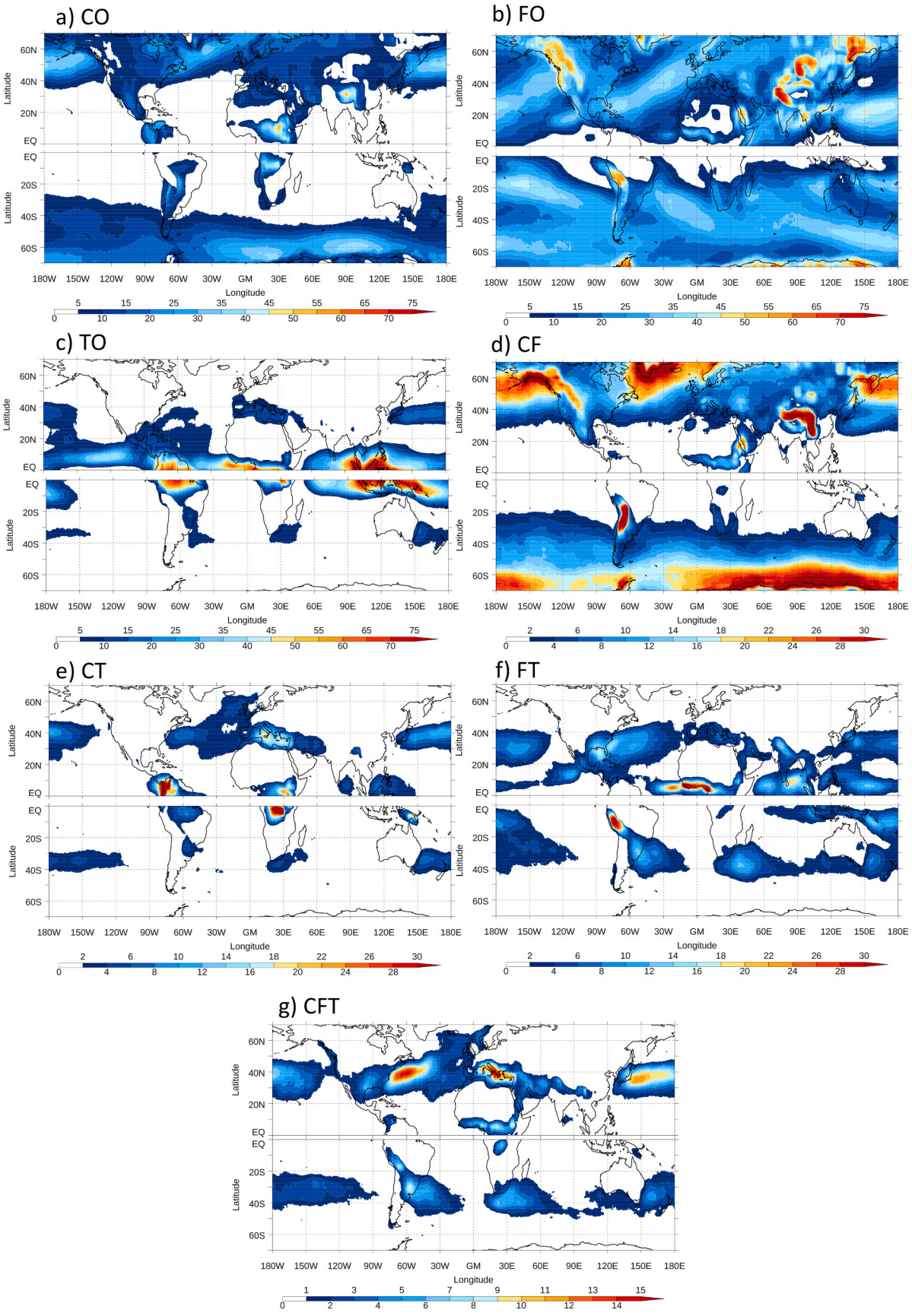

Fig. 4. Winter seasonal mean frequency of the different weather system types as a percentage of 6-hourly time points in the season. The weather system types are (a) CO, (b) FO, (c), TO, (d), CF, (e) CT, (f) FT, and (g) CFT. Note the different scales on the color bars for the single, double and triple weather system types. (For interpretation of the references to color in this figure legend, the reader is referred to the Web version of this article.)

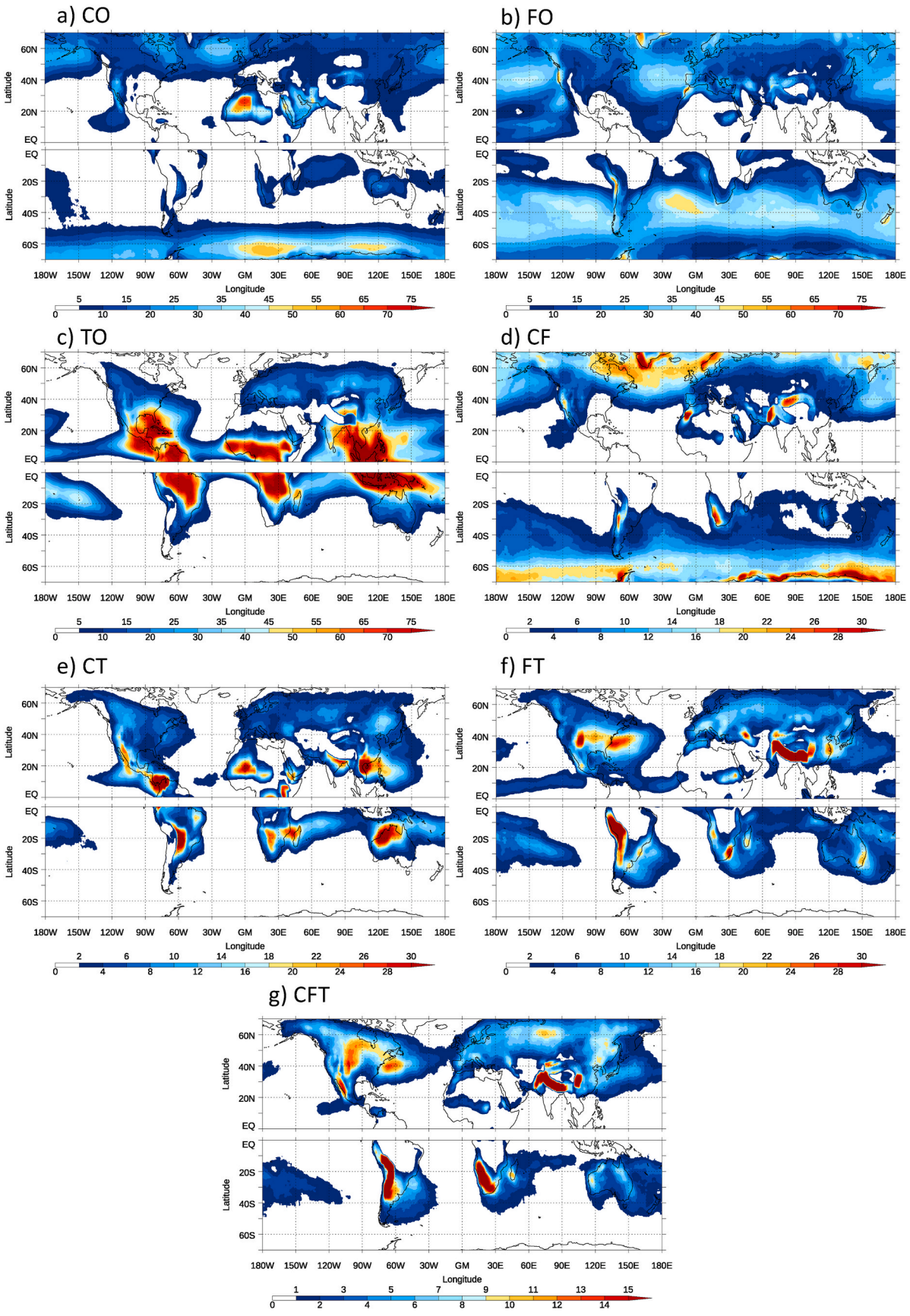

Fig. 5. As Fig. 4 but for summer.

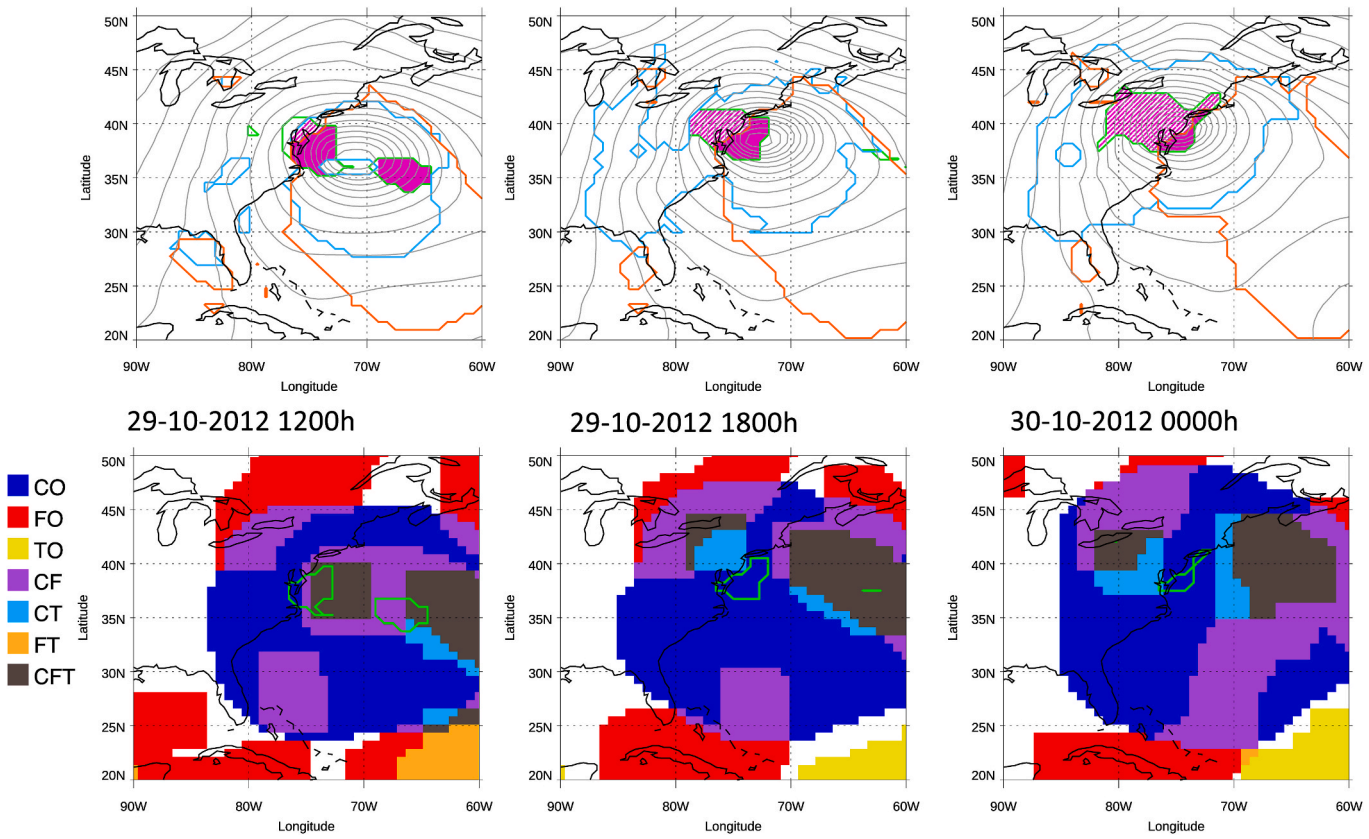

Fig. 6. Hurricane Sandy case study synoptic maps (top) and storm type (below). Top: Black contours show MSLP. Orange dotted contour shows region of extreme waves, light blue shows region of extreme wind, and green shows region of extreme precipitation. Regions where there is a "triple hazard'' are filled in magenta, while "double hazard'' (wind and precipitation) are hatched in magenta. Bottom: Storm types are shown by colors given in legend. In the bottom figures the green contour indicates the region of the triple hazard.

the October 29, 2012 at 12UTC to the 30th October at 00UTC, along with the type of hazard that was occurring, and the weather system types.

At 1200h on the October 29, 2012, the storm is already a very large feature, with extreme waves covering a very large area from the east coast of the U.S.A. out into the Atlantic. Over a large part of this region, the winds were also extreme. To the east and west of the storm center, there was also extreme precipitation, resulting in the triple hazard indicated for this region based on our method. Six hours later, the center of the storm is close to making landfall, and the triple hazard is confined to a region close to the coast, with the northern part being next to New York City. There is also a swath of land that is affected by joint extreme precipitation and winds. A further 6 h later (0000h October 30, 2012), the storm makes landfall and the impacts have penetrated further inland, giving a larger region of extreme wind and precipitation over land, and showing the triple hazard at the coast of New York City and New Jersey. This is when the largest impact—the storm surge—was seen.

The weather system types identified through the same period for Hurricane Sandy (Fig. 6) indicate a very large cyclone, within which are also other features. There are frontal structures to the north, south, and east of the cyclone, consistent with the extratropical transition of the hurricane, giving the CF storm type in parts of the storm. The triple weather system type (CFT) can also be seen, indicating thunderstorms near the center of the storm and along the front. There are also regions of CT, showing where thunderstorms are occurring without the presence of the front. The triple hazard (extreme precipitation, wind, and waves; indicated by the green contour) is located close to the location of the CFT region at 1200h, indicating the importance of this weather system type for the compound hazards. At the other times the triple hazard is located between two regions of CFT and CT weather system types in the center of the large cyclonic system.

The Pasha Bulker storm in June 2007 was an intense mid-latitude cyclone that impacted on eastern Australia and is one of Australia's most costly natural hazard events ever recorded (Mills et al., 2010). It is named after a ship that ran aground during that event due to the extreme wind and waves that occurred in a relatively small region of the central east coast, including recorded wind gusts of 135 km/h (Dowdy et al., 2019). Deep convective processes were evident for this event from examinations based on lightning observations (Dowdy and Kuleshov, 2014) and modeling (Chambers et al., 2014), as well as influences from a frontal system during the storm's development (Mills et al., 2010). These were driven by a strong upper level cut off low (Mills et al., 2010), in a similar way to other Australian east coast lows.

Fig. 7 shows the time evolution of the storm at 12 h intervals, along with the type of hazard that was occurring. A region with a compound hazard type of extreme precipitation and wind can be seen stretching from the ocean inland on the east coast, on the poleward side of the low pressure system. A very small region of the triple hazard can also be seen, which moves towards the coast during the three times shown, and is consistent with the region where the main storm damages occurred. At the first time shown, there is a large frontal cyclone with a front (likely a bent back warm front) stretching inland, and northwards along the coast. Convective activity is visible in the southern part of the cyclone (indicated by the CFT weather system type), and along the northward stretching front. At the second time shown, the convective activity is more indicated by the CT type. While the fronts are identified using our automated method, these were not analysed on the synoptic charts produced by the Australian Bureau of Meteorology at the time (Mills et al., 2010).

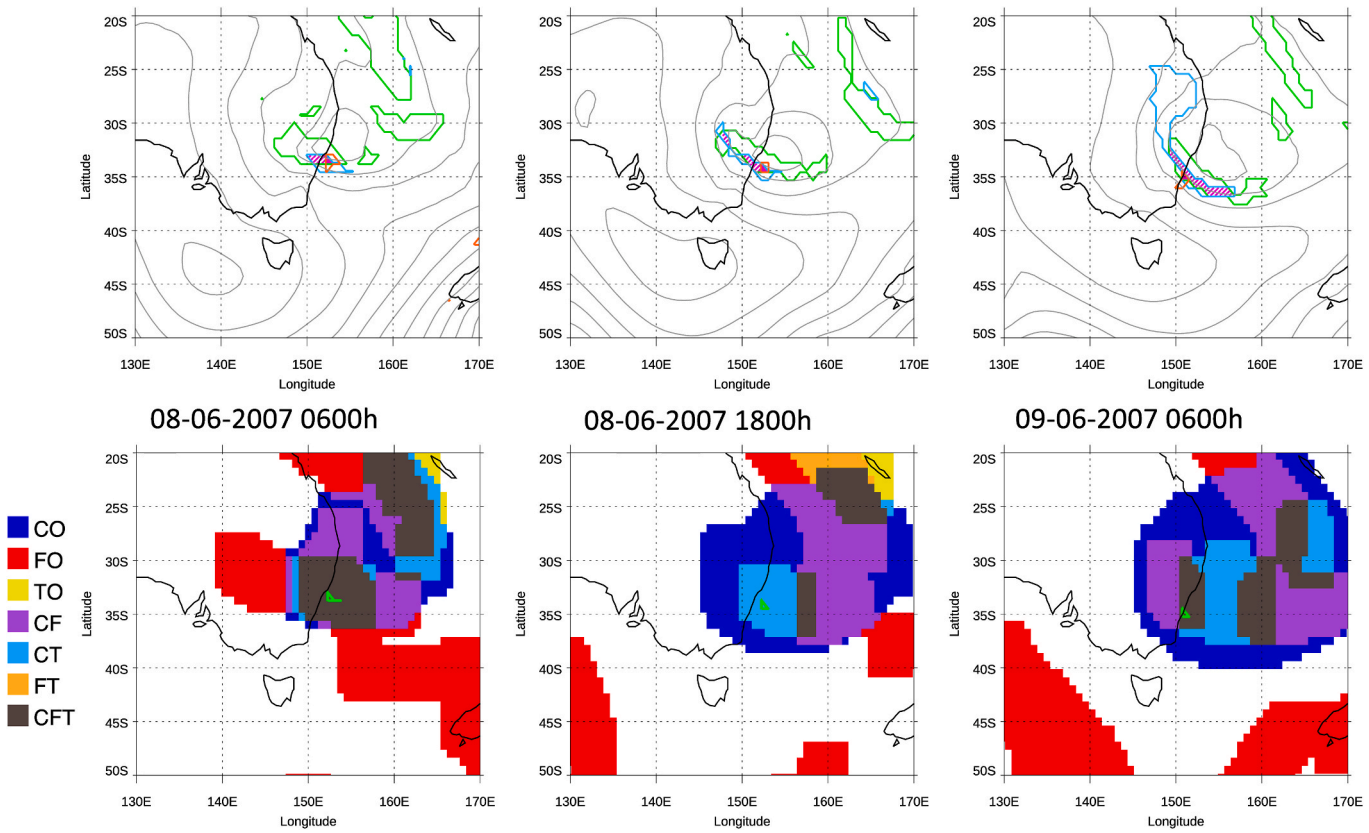

Fig. 7. As for Fig. 6 but for the Pasha Bulker case study. The 3 panels are now 12 h apart.

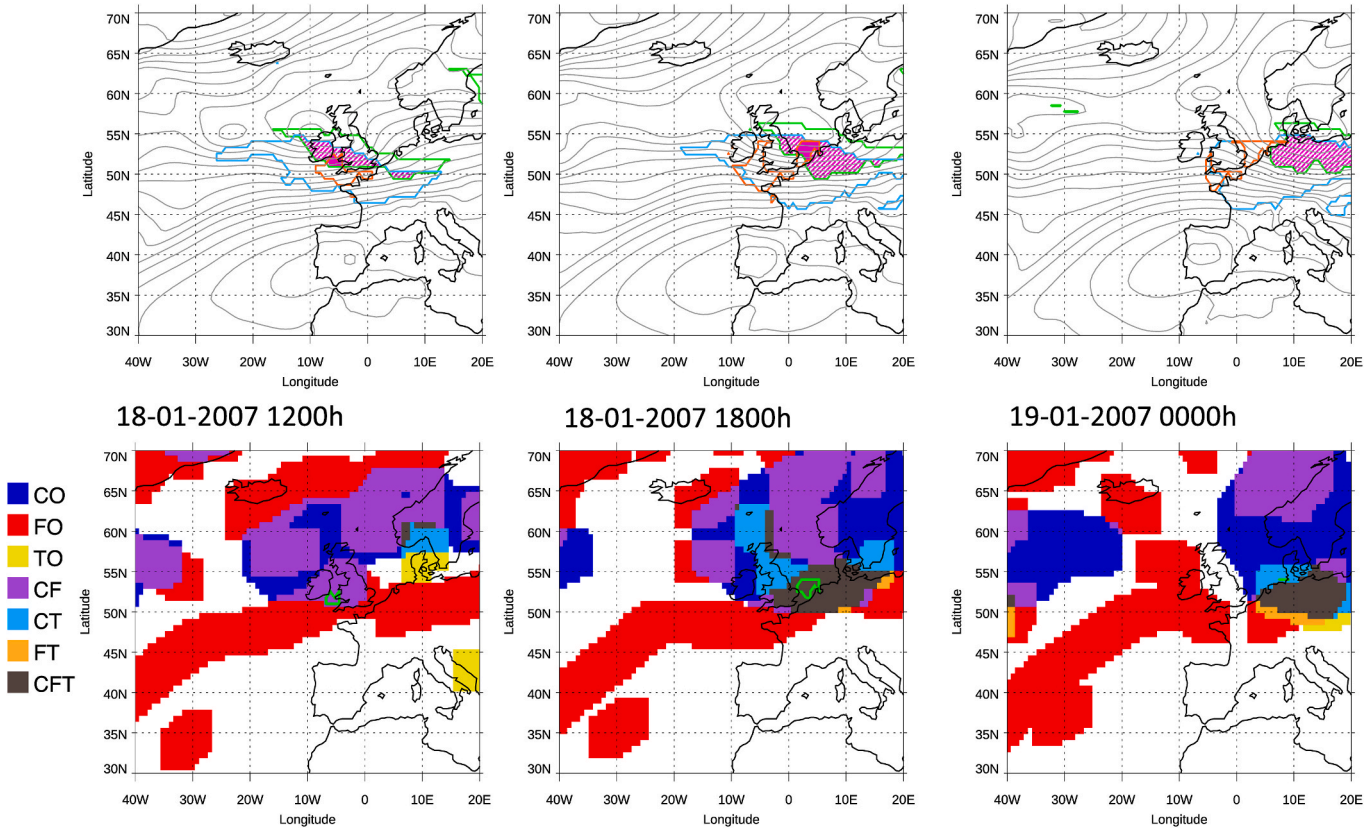

Fig. 8. As for Fig. 6 but for the storm Kyrill case study.

The double and triple hazards are located in the CFT weather system type in the warm frontal part of the storm at the first and last time steps shown, and then within the convective activity of the CT type in the second timestep. This is consistent with the previous analysis that indicated the deep convection and frontal influences associated with this storm's development and the intensity of the extreme weather that it caused.

European storm Kyrill (Fig. 8) is another example of a damaging extratropical cyclone (Fink et al., 2009). The synoptic situation at 1200h on January 18, 2007 shows a long frontal feature to the south of the UK, along with a wide cyclone region encompassing two low pressure centers. A small region in the Irish sea shows the triple hazard, while much of the south of the UK and Ireland show the joint extreme precipitation and winds. The extreme wind footprint is the largest hazard feature of this storm (Roberts et al., 2014). Six hours later, the extreme wind footprint is still very large but has moved over the European continent, and the triple hazard can now be seen in the North Sea off the coast of the Netherlands. By 0000h there is no longer a triple hazard visible, but the extreme precipitation and wind compound hazard covers a large region over the north of the European continent. The triple hazard in the 2nd time shown and the compound precipitation and wind extreme in the 3rd time are colocated with a triple storm (CFT).

The three cases shown indicate that the CFT weather system type may be important for the compound hazard types, including the triple hazard of extreme precipitation, wind, and waves. In the next section we will investigate the seasonal mean relationship over the 10-year period between the hazards and the storm types.

5.2. Seasonal mean link between hazards and weather system types

The main features of the link between extreme precipitation, wind, and wave events (and the compound events thereof) over the 10-year period can be summarized using zonal means of the frequency of the different hazards coincident with the seven weather system types (Fig. 9 and Fig. 10), which are similar to the figures shown in Dowdy and Catto (2017) for the single hazards of extreme precipitation and extreme winds. The results for extreme precipitation-only and wind-only are broadly similar to those presented in Dowdy and Catto (2017), while noting some variation due to the compound hazard types considered here. During winter (Fig. 9), extreme precipitation-only (Fig. 9a) is mostly associated with TO in the tropics between 10°S and 15°N. In the subtropics the main weather system type is FO, and polewards of 40°N and S the CF type is the most frequent, with FO and CO also occurring frequently. In the tropics and subtropics FT associated with extreme precipitation-only occurs up to 1% of the time. The CFT weather system type occurs with extreme precipitation-only around 30–40°N and S.

Extreme wind-only (Fig. 9b) also occurs most frequently with TO in the tropics, but with a lower overall frequency than extreme precipitation-only. The FO weather system type is the dominant weather system type over the rest of the NH and much of the SH up to around 60°S. CO and CF are similarly important over the mid-latitudes, while the CT, FT, and CFT show similar zonal mean patterns of frequency with

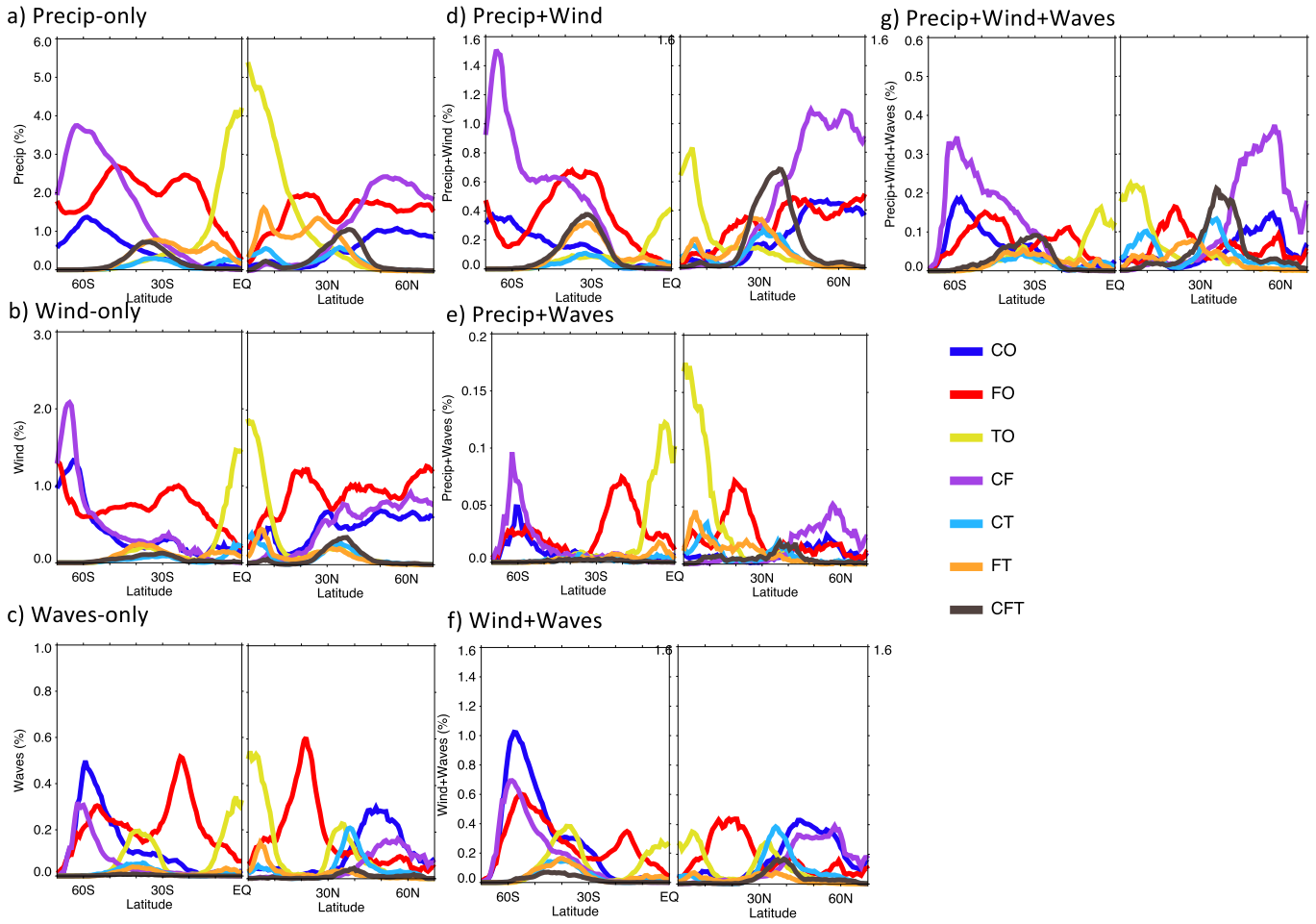

Fig. 9. Winter zonal mean frequency (% time) of hazards associated with different weather system types. The hazards shown are (a) extreme precipitation, (b) extreme wind gusts, (c) extreme waves, (d) compound extreme precipitation and wind gusts, (e) compound extreme precipitation and waves, (f) compound extreme wind gusts and waves, and (g) compound extreme precipitation, wind gusts, and waves. The colors for each weather system type is shown by the legend. (For interpretation of the references to color in this figure legend, the reader is referred to the Web version of this article.)

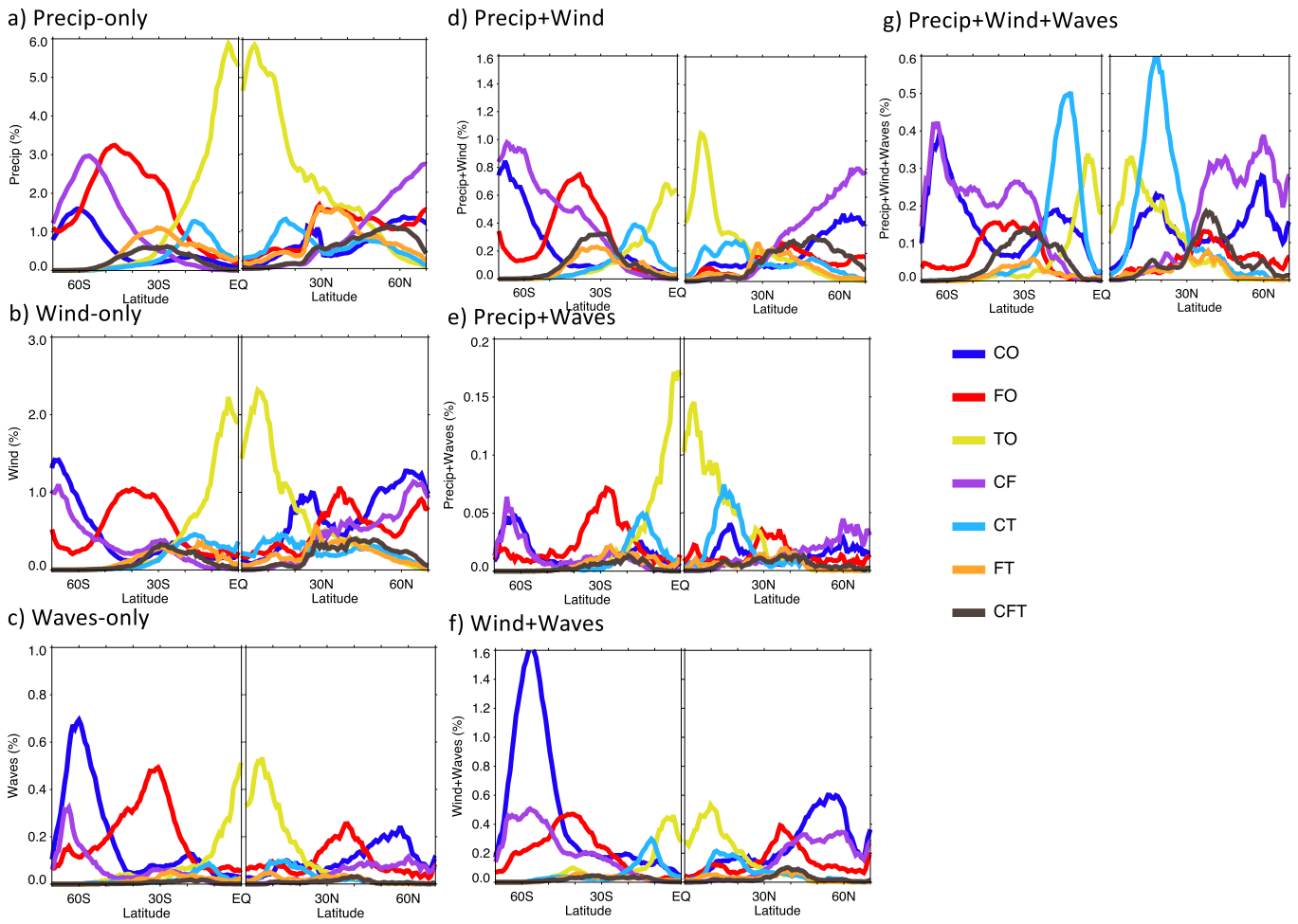

Fig. 10. As Fig. 9 but for summer.

extreme wind-only with peaks around 10°N and S and 30–40°N and S.

Extreme waves-only (Fig. 9c) show distinct peaks in the frequency associated with different weather system types. In the tropics the TO is dominant, but there are secondary peaks in the TO weather system type around 40°N and S. There are strong peaks in the frequency of FO related waves-only around 20°N and S, and peaks in the frequency of CO around 50–60°N and S. The CT type has a similar frequency to in the NH.

The zonal mean patterns for extreme precipitation and wind (Fig. 9d) show again that the highest frequency in the tropics is associated with the TO weather system type. CF is the most frequent polewards of 40°, as for the precipitation-only events (Fig. 9a). For this compound hazard we can see that there is much larger relative frequency of the combined weather-system types, especially the CFT, which has the highest frequency of all the weather system types around 30°N. FT also has a higher relative frequency than in the precipitation-only or wind-only events.

The frequency of extreme precipitation and wave events (Fig. 9e) is much lower than the other compound hazards, and the zonal mean patterns look very similar to the waves-only events, however without the second peak in TO seen at 40°N and S. This suggests that the presence of these compound hazards more closely resembles the waves-only features. We would expect that if we have extreme precipitation and extreme waves occurring together, that we would also have extreme winds, given the very strong relationship between extreme winds and waves and the physical link of the winds driving the waves. We have included this compound hazard for completeness and suggest that during these events there is likely some strong winds in order to generate the large waves. The compound extreme wind and waves occur in association with TO in the tropics, although with a much smaller peak than for the other hazards. They have similar frequencies associated with FO around 20°N and S, and with CO and CF in the mid-high latitudes. The CT type shows up in the NH around 35°N. The highest peak is in the SH around 50-60°S with high frequency of CO, FO and CF related extreme wind and waves.

The highest frequencies of the triple hazard of precipitation, wind and waves (Fig. 9g) occurs with the CF weather system type (up to 0.35%) between 50 and 60°N. They are also relatively frequent with the CFT weather system type around 30–40°N (up to 0.2% frequency).

To summarise the winter features, the TO is the most important weather system type for most of the hazards in the deep tropics, and CF is most important for precipitation-only, precipitation and wind, precipitation, wind and waves, and precipitation and waves events in the mid-high latitudes. FO is also very important over the subtropics for all of the hazards. Despite being less frequent than the double weather system types, the CFT type shows comparable importance for many of the hazards, and especially the combined extreme precipitation and wind, and the triple hazard. This is particularly true for the NH in the mid-latitudes (around 30–40°N) where it is equal to or exceeding the most common cause for triple hazard events. As shown in Fig. 4, this is associated with a clear pattern of high occurrence frequency for these triple weather system events around the east coasts of each continent through the world and adjacent maritime regions, as well as in the Mediterranean Sea.

During summer (Fig. 10), similar features can be seen so we will focus on the differences. For the precipitation-only hazard, the TO weather system dominates even more strongly in the tropics, and the peak associated with the ITCZ can be seen. There are peaks in the

frequency of precipitation-only associated with CT around 15°N and S, consistent with the high frequency of CT shown in Fig. 5. For the wind-only and wave-only events, there are similar frequencies as in winter, but the FO peak is at higher latitudes and the tropical TO band is wider. For extreme precipitation and wind events, there is also a higher frequency associated with CT, and the peak of this is well separated from the peak in FT and CFT, whereas in winter these three weather system types tend to peak around the same latitude. CT also features more strongly for the joint precipitation and waves and joint wind and waves events. The triple hazard events show a generally higher frequency in summer, with the highest frequencies associated with the CT weather system at 15°N and S. There is also a peak in the frequency associated with CO at similar latitudes, suggesting that these could also be tropical cyclone events but in a part of the storm without thunderstorm activity.

The global distribution of the most important weather system type for each hazard is shown for winter (Fig. 11) and summer (Fig. 12). This is defined as the weather system that accounts for the largest proportion of the hazard occurrences. A nine-point smoothing has been applied to the fields to provide a picture that is not as noisy. Some of the features of these maps are similar to those shown in Dowdy and Catto (2017), but with some differences associated with both the consideration of the compound hazards, and also the criteria for matching the hazards in space and time (shown in the supplementary material).

During winter, the extreme precipitation-only events, joint extreme precipitation and wind, and the triple hazard are most commonly associated with CF in the higher latitudes, FO in the mid-latitudes, and TO in the tropics, consistent with the zonal mean picture shown in Fig. 9. The spatial patterns show some interesting features, for example, the CT weather system type is the most common cause of these three hazard types over the southern Mediterranean and over the Atlantic Ocean close to the African coast. There is a band around 30°N where the CFT weather system type shows up as the most important type for the joint extreme precipitation and wind, and the triple hazard, with small regions in the west of the ocean basins where this is the most common weather system associated with the extreme precipitation alone. In the SH the CFT type is the most important for extreme precipitation-only and joint precipitation and wind just of the east coasts of the continents and for extreme wind-only to the east of South America. The FT type is also associated with these three hazards in similar regions to the CFT type, particularly over the warm waters of the western boundary currents.

The extreme wind-only events are mainly associated with the FO weather system type in winter over large parts of the globe, with smaller regions of CF, CO, CFT, and TO. This is similar to Dowdy and Catto (2017), but with a larger prevalence of the FO type associated mainly with the matching criteria for the hazards. The extreme wave-only and the joint wind and wave hazards show very similar patterns. Interestingly, there are regions in the mid-latitudes where the TO weather system type is the most common type for these hazards, which may be associated with the existence of swell waves propagating from further afield and is consistent with Fig. 9c. The joint extreme precipitation and wave events are less frequent and are associated with a mixture of weather system types, but mostly TO in the tropics, FO in the lower

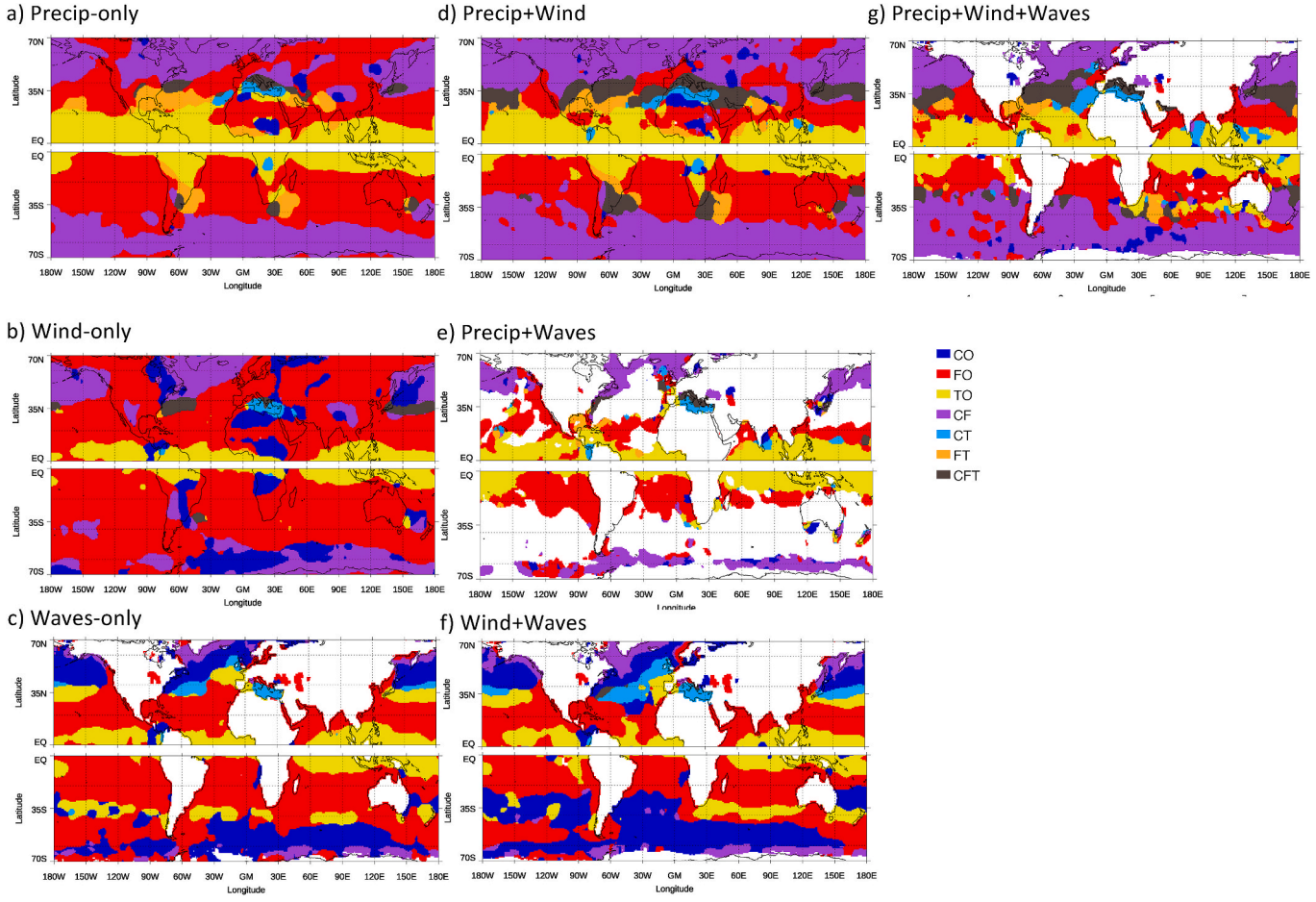

Fig. 11. Most common weather system type associated with the different hazards during winter in each hemisphere. The hazards shown are (a) extreme precipitation, (b) extreme wind gusts, (c) extreme waves, (d) compound extreme precipitation and wind gusts, (e) compound extreme precipitation and waves, (f) compound extreme wind gusts and waves, and (g) compound extreme precipitation, wind gusts, and waves. The colors for each weather system type are shown in the legend. (For interpretation of the references to color in this figure legend, the reader is referred to the Web version of this article.)

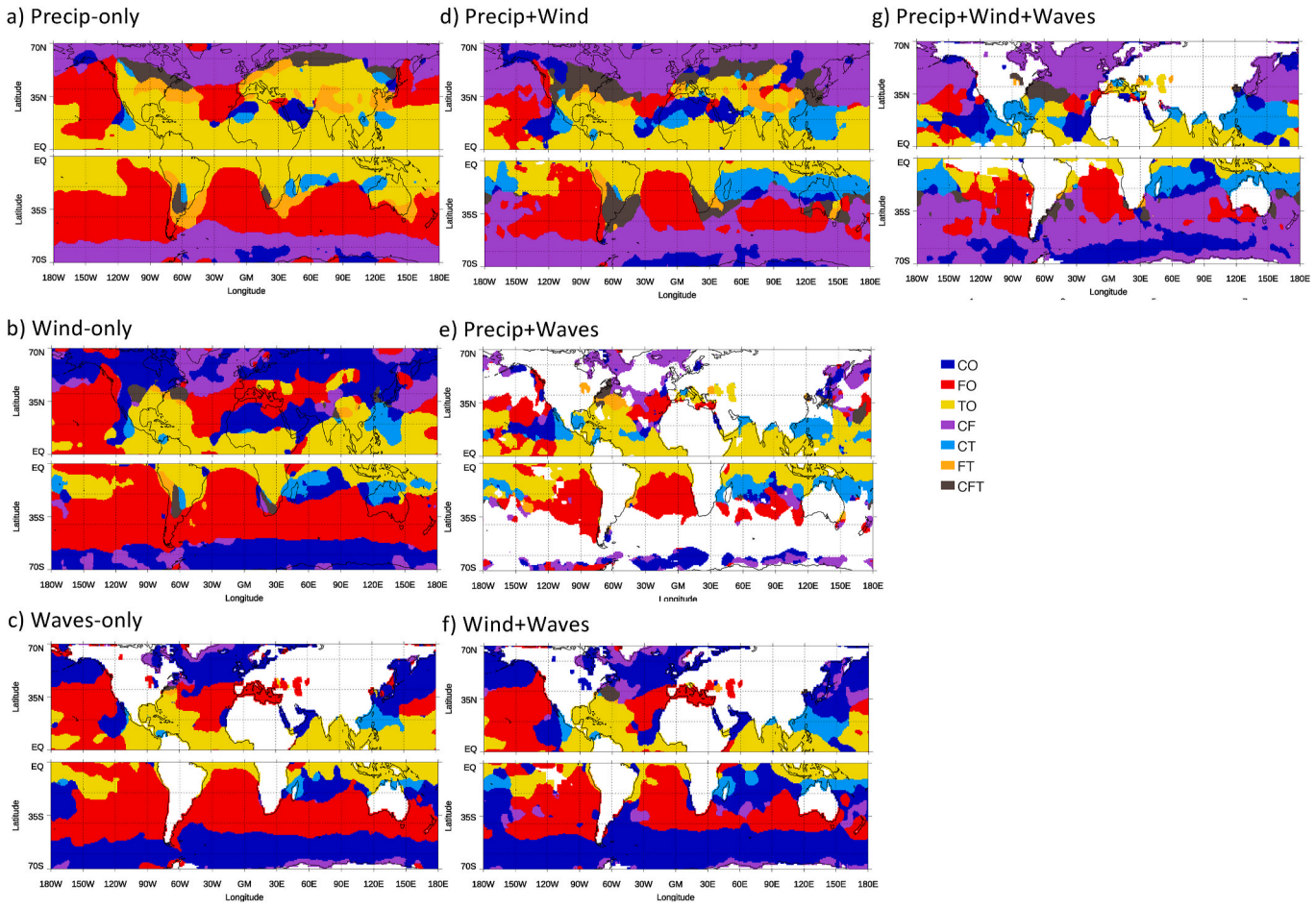

Fig. 12. As Fig. 11 but for summer in each hemisphere.

latitudes, and CF in the high latitudes.

During summer, many of the features are similar for the extreme precipitation-only, joint extreme precipitation and wind, and the triple hazard, however during summer there is a much bigger signal of the CT weather system type associated with tropical cyclones. There is also a poleward shift in and higher frequency over land of the location of the CFT most common feature. For the extreme wind-only, extreme wave-only, and joint extreme wind and waves, the CO and FO weather system types are the most important over high latitudes and mid-latitudes respectively. There are also regions where the CT type is the most common weather system type for these hazards, especially over the tropical cyclone regions of the NH and SH western Pacific and the southern Indian Ocean, and the west coast of central America.

The importance of the different weather system types for the occurrence of extreme hazards can be summarized using two different globally averaged metrics, shown in Fig. 13. The first tells us the proportion of each hazard type associated with each different weather system type (Fig. 13a and b), calculated by taking the total number of hazard events globally and calculating the probabilities that they occur with each different weather system type.

During winter, the largest proportion of extreme precipitation-only hazards are associated with the FO weather system type (approximately 25%), the second highest proportion from CF (20%). In fact, FO and CF are responsible for the largest proportions of all except waves-only and the joint extreme wind and waves (where CO is more important than CF). For the triple hazard, the CF type accounts for 25% of the hazards, while only approximately 6% is accounted for by each of the FT and CT types. In summer, TO accounts for the highest proportion of extreme precipitation-only events (19%), with FO almost as high. During summer (Fig. 13b), the CO weather system type accounts for more of the hazards than in the winter and the importance of the FO type is reduced. The triple hazard is mostly associated with CF (25% as in the winter), indicating there is not much seasonality in the occurrence of the CF type, while another 20% is accounted for by the CO type.

The second metric (Fig. 13c and d) is the probability of a hazard, given the presence of a certain weather system type, which is useful for the predictability and forecasting of the hazards. While FO is associated with a large proportion of the hazards (discussed above), the likelihood of getting an extreme event when the FO weather system type is present is relatively low. This concurs with the findings of Catto and Pfahl (2013) and is a consequence of the fronts themselves being a frequent feature. The probability of getting an extreme precipitation-only hazard is highest when the CFT weather system type is present at 29% during winter and 27% during summer. This is also the weather system type that is most likely to give a triple hazard during winter (5%), and the compound precipitation and wind events (13%) indicating the importance of this weather system type for extreme hazards including compound hazard types. During summer 7% of the CFT weather system type, and 6% of the CT type are associated with the triple hazard, and 9% of the CFT weather system types give compound extreme precipitation and wind.

6. Summary and discussion

Here we have investigated the occurrence frequency of individual and compound hazards of extreme precipitation, extreme wind gusts, and extreme wave heights. We have also systematically linked these hazards to the associated weather system types for the first time to

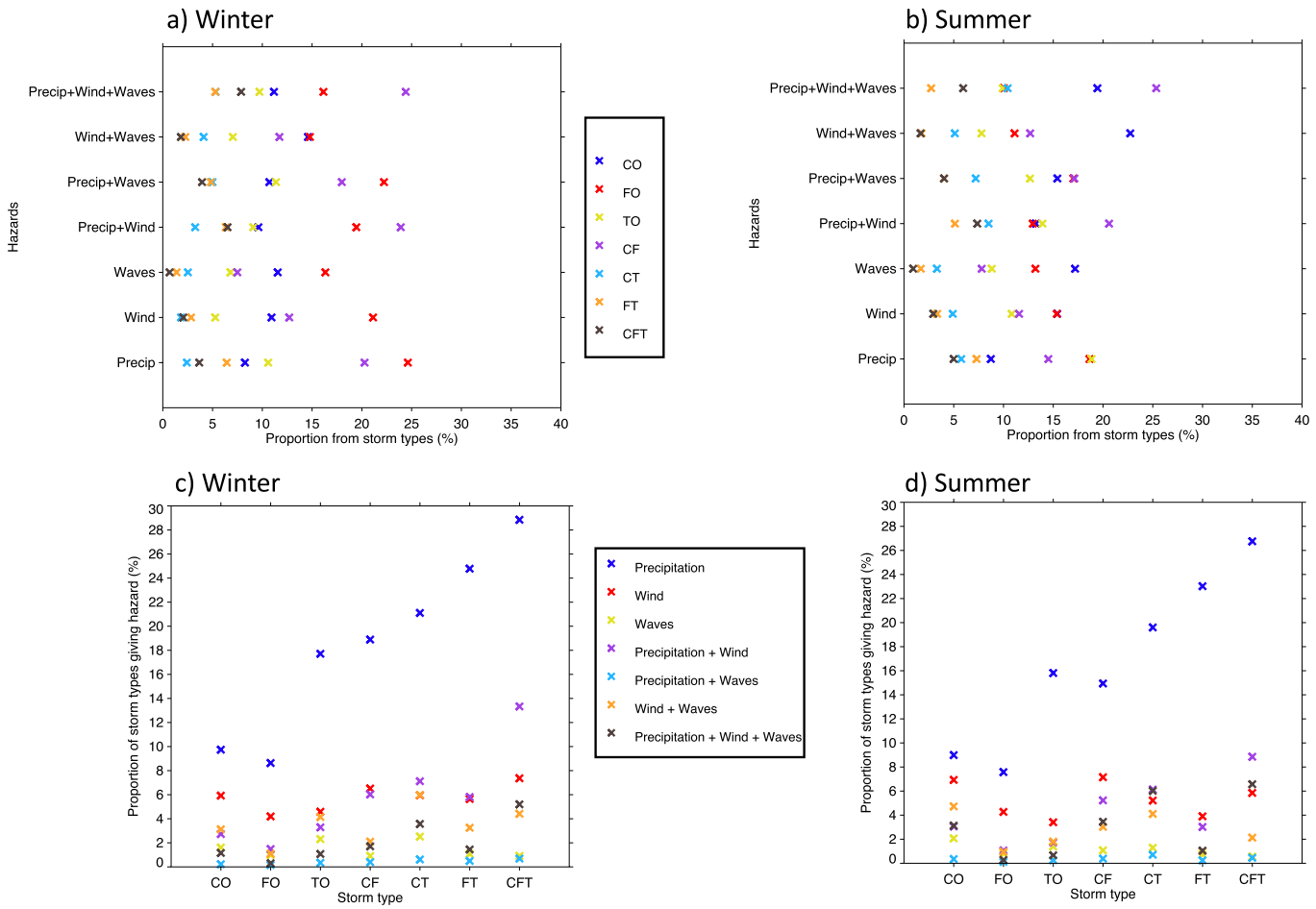

Fig. 13. Global mean proportion of hazards associated with the different weather system types (a, b) for (left) winter, and (right) summer, and probabilities of getting a hazard given the presence of the different weather system types (c, d).

determine the relative importance of each weather type for the impactful hazards.

The main conclusions from the study are as follows.

1. When considering the individual hazards, extreme precipitation-only and extreme wind-only events occur more frequently in isolation, with extreme precipitation-only occurring most frequently, up to 9% of the time in the mid-latitudes and up to 15% of the time in the deep tropics. The highest frequencies for extreme wind-only are over land (where they cannot be linked to waves).
2. Co-occurring extreme precipitation and wind events are quite common and occur more frequently during winter and mostly in the mid-latitudes. Co-occurring wind and waves are very common, and in many regions of the mid-latitudes occur more frequently than the extreme wind-only or waves-only.
3. The triple hazard of extreme precipitation, wind gusts and waves occurs most frequently over the Gulf Stream, the Kuroshio current and in the Mediterranean and occurs more frequently during summer in the tropical cyclone regions of the world.
4. The seasonal maps of weather system type frequencies highlight the different preferred regions for the individual and combined weather system types. CO occurs mostly in the highest latitudes, FO equatorwards of that, and TO mostly in the tropics. CF is mostly in the mid-latitudes as expected, and CT occurs during winter in the Mediterranean and the lower mid-latitudes, and in the summer highlights regions of tropical cyclones.
5. The case studies highlight the co-location of the triple hazard with the CFT weather type close to the center of an extratropical cyclone (or post-tropical cyclone).
6. The most common cause of many of the hazards in the mid-latitudes tends to be the CF weather type, with a large importance of FO. For wave-related hazards, FO and CO are more commonly associated. The CFT weather system type is important in both winter and summer for many of the hazards in the lower mid-latitudes, especially where the underlying SSTs are higher. In the tropics in winter the most common cause of most hazards is the TO type, and in the summer there is a high importance of the CT type, indicating tropical cyclones.
7. Considering the likelihood of getting a hazard given a certain weather system type, in a global average sense the CFT type gives the highest probability.

The compound event framework used here allow a number of aspects to be examined, particularly around the interrelationships between the different extreme event types. The high frequency of compound wind and wave extremes, for example, suggests either that there is a causality present, or that they are both produced by the same meteorological feature (which in this case included consideration of a range of different weather system types comprising different combinations of cyclones, fronts and thunderstorms). If the likelihood of the joint extreme (relative to the individual extremes) is unchanged for the different weather system types, this suggests a potential causality (i.e. a common physical process causing both types of hazard). Here, an example of this is the compound wind and waves. The percentage of all extreme wave events

during winter that are compound wind and waves events is highest for the CO weather system type at 57%, and lowest for the CFT type at 37%, but for most of the weather system types the values are between 40 and 50%. The relatively small changes between the weather system types suggests that there is causality in this compound hazard - likely the strong winds causing the extreme waves. Whereas, if the likelihood of the compound extreme is higher for certain weather system types (relative to the individual events), then this indicates that the individual meteorological conditions are important to consider for each hazards type. An example for this is the compound extreme precipitation and wind events. The percentage of extreme precipitation events that are compound extreme precipitation and winds is only 10% for the TO weather system type, but 32% for the CFT type and 25% for the CF type. Both the precipitation and wind hazards are caused by the same weather systems. This result is consistent with the findings of Owen et al., 2021.

Many of the hazards do not show much seasonality (bearing in mind that the extremes are defined separately for each season), other than the triple hazard and extreme wind-only (which occurs more frequently in summer) and the co-occurring extreme precipitation and winds (which occurs more frequently in winter than summer). The less frequent precipitation and wind events in summer is most likely associated with the decrease in the frequency of cyclones and fronts in that season (Hoskins and Hodges, 2002; Catto et al., 2012). Since these storm systems provide a mechanism by which the precipitation and winds can co-occur, without them the extreme events are occurring separately (since the percentile threshold means there are the same number of extreme times at each grid box). There is a much higher frequency of wind-only events over land during summer, which suggests dry convective activity producing strong wind gusts (e.g. Knippertz et al., 2007).

Previous studies have shown that extreme waves tend to occur in the cold conveyor belt region of extratropical cyclones (Bell et al., 2016). This would likely be on the poleward side of the warm front, which is consistent with the case studies presented here. The position within an extratropical cyclone is important for considering whether or not an extreme event might occur. For example, Catto et al. (2015) showed that fronts are more likely to produce extreme precipitation if they are linked with a warm conveyor belt. The different preferred locations of extreme waves, winds and precipitation within extratropical cyclones, suggests that hazards that occur independently in our analysis, may actually occur at the same time in different regions of the weather system. For example, Raveh-Rubin and Wernli (2015) find a temporal lag between extreme precipitation and extreme wind in the Mediterranean for events that are clearly associated with an individual weather system. This is worth investigating further using a Lagrangian feature tracking method, since it may still be important for insurance or reinsurance industries to know when multiple extremes occur at the same time in different locations.

The mid-latitude east coast regions of each continent of the world and the Mediterranean Sea are locations where intense cyclones can occur, including subtropical systems that can have significant influences from both tropical and extratropical energy sources for their genesis (Yanase and Niino, 2015; Quinting et al., 2019b; da Rocha et al., 2018; Dowdy et al., 2019; Quinting et al., 2019a). In order to better understand the hazard potential of different weather systems, the consideration of compound extremes is important. Here we show the strong relationship between extreme wind and waves, which could help in the understanding of the joint distributions and the economic losses suggested by Ye and Fang (2018).

In this study we are considering only extreme events that occur in a 6 h period. In terms of precipitation accumulations, these would be considered on the long end of the short-duration event classification (Breugem et al., 2020). There are many precipitation characteristics that would be important when considering the likelihood of them causing flooding events, such as duration and spatial extent. An investigation of these characteristics and how they relate to weather system types would be an interesting area of future study.

We acknowledge that there are many methods that can be used to identify fronts and cyclones, and thunderstorms, and the numerical results of the study would likely be somewhat different if other methods were used. However, what we focus on here is the interpretation of the results that we find based on this approach with the aim of providing new insight on the interrelationships between these compound hazard and compound weather system types.

Declaration of competing interest

The authors declare that they have no known competing financial interests or personal relationships that could have appeared to influence the work reported in this paper.

Acknowledgments

JLC was partly funded by the Natural Environment Research Council (NERC) EMERGENCE of Climate Hazards grant (NE/S004645/1) and STORMY-WEATHER grant (NE/V004166/1). AD was supported through the Earth Systems and Climate Change (ESCC) Hub of the Australian Government's National Environmental Science Program (NESP). ERA-Interim data are available online(http://apps.ecmwf.int/datasets/).

Appendix A. Supplementary data

Supplementary data to this article can be found online at https://doi.org/10.1016/j.wace.2021.100313.

Author statement

Jennifer L Catto: Conceptualization, Methodology, Software, Writing - original draft preparation, Visualisation, Investigation

Andrew Dowdy: Conceptualization, Data curation, Software, Investigation, Writing – Reviewing and editing.

References

Bell, R.J., Gray, S.L., Jones, O.P., 2016. North Atlantic storm driving of extreme wave heights in the North Sea. J. Geophys. Res. Oceans 122, 3253–3268. https://doi.org/10.1002/2016JC012501.

Berry, G., Reeder, M.J., Jakob, C., 2011. A global climatology of atmospheric fronts. Geophys. Res. Lett. 38 https://doi.org/10.1029/2010GL046451.

Bevacqua, E., Maraun, D., Vousdoukas, M.I., Voukouvalas, E., Vrac, M., Mentaschi, L., Widmann, M., 2019. Higher probability of compound flooding from precipitation and storm surge in Europe under anthropogenic climate change. Sci. Adv. 5 (9) https://doi.org/10.1126/sciadv.aaw5531.

Bevacqua, E., Vousdoukas, M.I., Zappa, G., Hodges, K.I., Shepherd, T.G., Maraun, D., Mentaschi, L., Feyen, L., 2020. More meteorological events that drive compound coastal flooding are projected under climate change. Communications Earth & Environ 1 (47). https://doi.org/10.1038/s43247-020-00044-z.

Breugem, A.J., Wesseling, J.G., Oostindie, K., Ritsema, C.J., 2020. Meteorological aspects of heavy precipitation in relation to floods – an overview. Earth Sci. Rev. https://doi.org/10.1016/j.earscirev.2020.103171.

Catto, J.L., Jakob, C., Berry, G., Nicholls, N., 2012. Relating global precipitation to atmospheric fronts. Geophys. Res. Lett. 39 https://doi.org/10.1029/2012GL051736.

Catto, J.L., Jakob, C., Nicholls, N., 2015. Can the CMIP5 models represent winter frontal precipitation? Geophys. Res. Lett. 42, 8596D8604. https://doi.org/10.1002/2015GL066015.

Catto, J.L., Pfahl, S., 2013. The importance of fronts for extreme precipitation. J. Geophys. Res. 118 (10), 791. https://doi.org/10.1002/jgrd.50852.

Chambers, C.R.S., Brassington, G.B., Simmonds, I., Walsh, K., 2014. Precipitation changes due to the introduction of eddy-resolved sea surface temperatures into simulations of the "Pasha Bulker" east coast low of June 2007. Meteorol. Atmos. Phys. 125, 1–15. https://doi.org/10.1007/s00703-014-0318-4.

da Rocha, R.P., Reboita, M.S., Gozzo, L.F., Dutra, L.M.M., de Jesus, E.M., 2018. Subtropical cyclones over the oceanic basins: a review. Ann. N. Y. Acad. Sci. 1436, 138–156. https://doi.org/10.1111/nyas.13927.

De Luca, P., Messori, G., Pons, F.M.E., Faranda, D., 2020. Dynamical systems theory sheds new light on compound climate extremes in europe and eastern north America. Q. J. R. Meteorol. Soc. 146 (729), 1636–1650. https://doi.org/10.1002/qj.3757.

Dee, D.P., Coauthors, 2011. The ERA-Interim reanalysis: configuration and performance of the data assimilation system. Quart. J. Roy. Meteor. Soc. 137, 553–597.

Dowdy, A., Catto, J.L., 2017. Extreme weather caused by concurrent cyclone, front and thunderstorm occurrences. Sci. Rep. 7 https://doi.org/10.1038/srep40359.
Dowdy, A.J., Kuleshov, Y., 2014. Climatology of lightning activity in Australia: spatial and seasonal variability. Aust. Meteor. Ocean J. 64, 103–108.
Dowdy, A.J., Coauthors, 2019. Review of Australian east coast low pressure systems and associated extremes. Clim. Dynam. 53, 4887–4910. https://doi.org/10.1007/s00382-019-04836-8.
Fink, A.H., Brücher, T., Ermert, V., Krüger, A., Pinto, J.G., 2009. The European storm Kyrill in January 2007: synoptic evolution, meteorological impacts and some considerations with respect to climate change. Nat. Hazards Earth Syst. Sci. 9, 405–423.
Galarneau Jr., J, T., Davis, C.A., Shapiro, M.A., 2013. Intensification of hurricane Sandy (2012) through extratropical warm core seclusion. Mon. Weather Rev. 141, 4296–4321. https://doi.org/10.1175/MWR-D-13-00181.1.
Hewson, T.D., 1998. Objective fronts. Meteorol. Appl. 5, 37–65.
Hoskins, B.J., Hodges, K.I., 2002. New perspectives on the Northern Hemisphere winter storm tracks. J. Atmos. Sci. 59, 1041–1061.
Hénin, R., Ramos, A.M., Pinto, J.G., Liberato, M.L.R., 2020. A ranking of concurrent precipitation and wind events for the Iberian Peninsula. Int. J. Climatol. https://doi.org/10.1002/joc.6829.
Knapp, K.R., Kruk, M.C., Levinson, D.H., Diamond, H.J., Neumann, C.J., 2010. The international best track archive for climate stewardship (iBTrACS). Bull. Am. Meteorol. Soc. 91, 363–376. https://doi.org/10.1175/2009BAMS2755.1.
Knippertz, P., Deutscher, C., Kandler, K.,-ller, T.M.", Schulz, O., Sch, L.,-tz, 2007. Dust mobilization due to density currents in the Atlas region: observations from the Saharan Mineral Dust Experiment 2006 field campaign. J. Geophys. Res. 112, D21–D109. https://doi.org/10.1029/2007JD008774.
Komen, G.J., Cavaleri, M., Donelan, M., Hasselmann, K. (Eds.), 1994. Modelling of Ocean Waves. Cambridge University Press, New York, p. 532.
Kunkel, K.E., Easterling, D.R., Kristovich, D.A.R., Gleason, B., Stoecker, L., Smith, R., 2012. Meteorological causes of the secular variations in observed extreme precipitation events for the conterminous United States. J. Hydrometeorol. 13, 1131–1141.
Liberato, M.L.R., Pinto, J.G., Ludwig, P., ordonez, P., Yuen, D., Trigo, I.F., 2013. Explosive development of winter storm Xynthia over the subtropical North Atlantic ocean. Nat. Hazards Earth Syst. Sci. 13, 2239–2251. https://doi.org/10.5194/nhess-13-2239-2013.
Liu, B., Siu, Y.L., Mitchell, G., 2016. Hazard interaction analysis for multi-hazard risk assessment: a systematic classification based on hazard-forming environment. Nat. Hazards Earth Syst. Sci. 16 (2), 629–642. https://doi.org/10.5194/nhess-16-629-2016. https://nhess.copernicus.org/articles/16/629/2016/.
Martius, O., Pfahl, S., Chevalier, C., 2016. A global quantification of compound precipitation and wind extremes. Geophys. Res. Lett. 43, 7709–7717. https://doi.org/10.1002/2016GL070017.
Mills, G.A., Webb, R., Davidson, N.E., Kepert, J., Seed, A., Abbs, D., 2010. The Pasha Bulker east coast low of 8 June 2007. Tech. Rep. 23. http://www.cawcr.gov.au/publications/technicalreports.php. Centre for Australia Weather and Climate Research. URL,.
O'Brien, L., Renzi, E., Dudley, J.M., Clancy, C., Dias, F., 2018. Catalogue of extreme wave events in Ireland: revised and updated for 14?680 BP to 2017. Nat. Hazards Earth Syst. Sci. 18, 729–758. https://doi.org/10.5194/nhess-18-729-2018.
Owen, L.E., Catto, J.L., Stephenson, D.B., Dunstone, N., 2021. Compound precipitation and wind extremes over Europe and their relationship to extratropical cyclones. Weather. Clim. Extremes (submitted for publication).
Pfahl, S., Wernli, H., 2012. Quantifying the relevance of cyclones for precipitation extremes. J. Clim. 25, 6770–6780.
Quinting, J.F., Catto, J.L., Reeder, M.J., 2019a. Synoptic climatology of hybrid cyclones in the Australian region. Quart. J. Roy. Meteor. Soc. 145.
Quinting, J.F., Reeder, M.J., Catto, J.L., 2019b. The intensity and motion of hybrid cyclones in the Australian region in a composite potential vorticity framework. Quart. J. Roy. Meteor. Soc. 145.
Raveh-Rubin, S., Wernli, H., 2015. Large-scale wind and precipitation extremes in the Mediterranean: a climatological analysis for 1979-2012. Quart. J. Roy. Meteor. Soc. 141, 2404–2417. https://doi.org/10.1002/qj.2531.
Roberts, J.F., Coauthors, 2014. The XWS open access catalogue of extreme European windstorms from 1979 to 2012. Nat. Hazards Earth Syst. Sci. 14, 2487–2501. https://doi.org/10.5194/nhess-14-2487-2014.
Semedo, A., Sušelj, K., Rutgersson, A., Sterl, A., 2011. A global view on the wind sea and swell climate and variability from ERA-40. J. Clim. 24 (5), 1461–1479. https://doi.org/10.1175/2010JCLI3718.1.
Seneviratne, S.I., Coauthors, 2012. In: Field, C.B., Barros, V., Stocker, T.F., Qin, D., Dokken, D.J., Ebi, K.L., Mastrandrea, M.D., Mach, K.J., Plattner, G.-K., Allen, S.K., Tignor, M., Midgley, P.M. (Eds.), Managing the Risks of Extreme Events and Disasters to Advance Climate Change Adaptation, *A Special Report of Working Groups I and II of the Intergovernmental Panel on Climate Change (IPCC)*, Chap. Changes in Climate Extremes and Their Impacts on the Natural Physical Environment, vols. 109–230. Cambridge University Press, Cambridge, UK, and New York, NY, USA.
Utsumi, N., Kim, H., Kanae, S., Oki, T., 2017. Relative contributions of weather systems to mean and extreme global precipitation. J. Geophys. Res. 122, 152–167.
van den Hurk, B., van Meijgaard, E., de Valk, P., van Heering, K.-J., Gooijer, J., 2015. Analysis of a compounding surge and precipitation even in The Netherlands. Environ. Res. Lett. 10 https://doi.org/10.1088/1748-9326/10/3/035001.
Virts, K.S., Wallace, J.M., Hutchins, M.L., Holzworth, R.H., 2013. Highlights of a new ground-based, hourly global lightning climatology. Bull. Am. Meteorol. Soc. 94, 1381–1391. https://doi.org/10.1175/BAMS-D-12-00082.1.
Wernli, H., Schwierz, C., 2006. Surface cyclones in the ERA-40 dataset (1958-2001). Part I: novel identification method and global climatology. J. Atmos. Sci. 63, 2486–2507.
Wu, W., McInnes, K., O'Grady, J., Hoeke, R., Leonard, M., Westra, S., 2018. Mapping dependence between extreme rainfall and storm surge. J. Geophys. Res. Oceans 123, 313–317.
Yanase, W., Niino, H., 2015. Idealized numerical experiments on cyclone development in the tropical, subtropical and extratropical environments. J. Atmos. Sci. 72, 3699–3714. https://doi.org/10.1175/JAS-D-15-0051.1.
Ye, Y., Fang, W., 2018. Estimation of the compound hazard severity of tropical cyclones over coastal China during 1949–2011 with copula function. Nat. Hazards 93, 887–903. https://doi.org/10.1007/s11069-018-3329-5.
Zheng, F., Westra, S., Leonard, M., Sisson, S.A., 2014. Modeling dependence between extreme rainfall and storm surge to estimate coastal flooding risk. Water Resour. Res. 50 (3), 2050–2071. https://doi.org/10.1002/2013WR014616.
Zscheischler, J., Seneviratne, S., 2017. Dependence of drivers affects risks associated with compound events. Science Advances 3. https://doi.org/10.1126/sciadv.1700263.
Zscheischler, J., Coauthors, 2018. Future climate risk from compound events. Nat. Clim. Change 8, 469–477. https://doi.org/10.1038/s41558-018-0156-3.